UPPSALA
UNIVERSITET

UPTEC X 19 044
Examensarbete 30 hp
November 2019

Production and harvesting of volatile jet fuel precursors from *Synechocystis* sp. PCC 6803

Johan Sjölander

UPPSALA
UNIVERSITET

Teknisk- naturvetenskaplig fakultet
UTH-enheten

Besöksadress:
Ångströmlaboratoriet
Lägerhyddsvägen 1
Hus 4, Plan 0

Postadress:
Box 536
751 21 Uppsala

Telefon:
018 – 471 30 03

Telefax:
018 – 471 30 00

Hemsida:
http://www.teknat.uu.se/student

Abstract

Production and harvesting of volatile jet fuel precursors from *Synechocystis* sp. PCC 6803

Johan Sjölander

The world is currently faced with the enormous challenge of slowing down human triggered global warming. As the global energy demand increases, there is an urgent need for renewable and carbon-neutral fuel-sources. Isoprene and isobutene are crude-oil derived, short, volatile and reactive hydrocarbons that can be polymerised into longer chains to be used as jet fuel. Isoprene has previously been produced from the cyanobacterial strain *Synechocystis* sp. PCC 6803 but there has been no reported isobutene synthesis from any photosynthetic organism. This work aimed to synthesise isobutene in *Synechocystis* using a cytochrome P450 from *Cystobasidium minutum* with reported isobutene production capability. Substrate availability was to be provided through the insertion of two heterologous enzymes, IpdC from *Salmonella typhimurium* and PadA from *Escherichia coli*. Both IpdC and PadA were successfully expressed in *Synechocystis* but the functional activities of IpdC, PadA and the cytochrome P450 in *Synechocystis* remains undetermined. This project also had the aim to design and construct a photo-bioreactor and gas collection system capable of producing and harvesting isoprene directly from an engineered *Synechocystis* strain. Herein lies a description of a closed system photobioreactor connected to a cold-trap that was able to concentrate isoprene produced from *Synechocystis* to measurable amounts.

Handledare: Karin Stensjö
Ämnesgranskare: Gunnar Johansson
Examinator: Jan Andersson
ISSN: 1401-2138, UPTEC X 19 044

Sammanfattning

Världen lider just nu av allvarliga konsekvenser på grund av den globala uppvärmningen orsakad av människan. Den totala energiförbrukningen ökar i en oroväckande takt medan de fossila energikällorna sinar. Det finns ett enormt och brådskande behov av hållbara energikällor som inte släpper ut växthusgaser i atmosfären. Många ser sol- och vindkraft som en bra lösning på detta problem. Idag används dock dessa energikällor främst för elektricitet- och värmeproduktion trots att större delen av världens energikonsumtion består av förbränning av bränsle. Solens potential som framtidens energikälla slutar dock inte där. En av jordens viktigaste kemiska processer, fotosyntesen, använder solens energi för att omvandla vatten och koldioxid till kolväten och syre. Fotosyntesen utnyttjas av en mängd olika organismer som växter, alger och till och med bakterier som kallas för cyanobakterier. De kolväten som produceras i cellerna hos dessa bakterier används som en intern energikälla. Forskare världen över har nyligen öppnat ögonen för möjligheten att genetiskt manipulera cyanobakterier för att omdirigera produktionen av kolväten mot andra användbara ämnen som till exempel bränslen.

Isobuten och isopren är korta, flyktiga kolväten som i stor utsträckning används för att syntetisera gummi och diverse tillsatser som förbättrar bensinkvalitet. Med hjälp av solljus kan dessa korta kolväten sättas ihop till längre kolväten som kan användas som jetbränsle. Jetbränsle är av högre kvalitet än till exempel bensin och kan innehålla kolväten med 8 till 17 kolatomer. Idag tillverkas isobuten och isopren nästan uteslutande från krackning av råolja och det finns ingen kommersiell produktion av dessa molekyler från cyanobakterier eller andra fotosyntetiserande organismer. Forskare har tidigare lyckats med att syntetisera isopren från cyanobakterien *Synechocystis* sp. PCC 6803 men processen är ännu inte ekonomiskt gynnsam för industrin. Det finns ett behov av effektiva metoder för odling av bakterier och uppfångning av den gas som bakterierna producerar så att de kan polymeriseras till bränsle.

Detta projekt hade två huvudmål. Ett av målen var att utveckla en s.k. fotobioreaktor och ett system för att fånga gas. Syftet med det var att utvärdera möjligheterna att direkt fånga isopren som produceras av cyanobakterier. Här beskrivs ett slutet fotobioreaktorsystem kopplat till en köldfälla som kunde koncentrera isopren som hade producerats av *Synechocystsis* till mätbara mängder. Det andra målet var att genetiskt modifiera *Synechocystis* så att bakterien tillverkar enzymer som arbetar tillsammans för att syntetisera isobuten. Dessa enzymer undersöktes separat i både modellorganismen *Eschereshia coli* och *Synechocystis.* Alla enzymer kunde påvisas i dessa organismer men deras aktiviteter kunde inte bestämmas.

Index

Abbreviations

BCD	Bi-cistronic design
β-DM	n-dodecyl-beta-maltoside detergent
CBB	Calvin-Benson-Bassham
GC	Gas Chromatography
GC-MS	Gas chromatography mass spectrometry
Cyt.P450cm	Cytochrome P450 from *Cystobasidium minutum*
DCM	Dichloromethane
DMAPP	Dimethylallyl pyrophosphate
DTT	Ditiotreitol
DXS	1-deoxy-D-xylulose-5-phoshphate synthase
EVC	Empty vector control
FID	Flame ionization detector
HRP	Horseradish peroxidase
IpdC	Indolepyruvate decarboxylase from *Salmonella typhimurium*
IPI	Isopentenyl diphosphate
IPP	Isopentenyl pyrophosphate
IspS	Isoprene synthase
LC-MS	Liquid Cromatography – Mass Spectrometry
MEP	2-C-methyl-D-erythritol 4-phosphate
M3K	Mevalonate-3-kinase
OD	Optical density
PadA	Phenylacetaldehyde dehydrogenase from *Escherichia coli*

PBQ	Phenyl-p-benzoquinone
SDS	Sodium dodecyl sulfate
Synechocystis	*Synechocystis* sp. PCC 6803
PAGE	Polyacrylamide gel electrophoresis
PBR	Photobioreactor
PCR	Polymerase chain reaction
PSI	Photosystem I
PSII	Photosystem II
PTFE	Polytetrafluoroethylene
PVDF	Polyvinylidene fluoride
WT	Wild type

1 Introduction

The world is currently struggling to deal with the escalating consequences associated with human triggered global warming. Recently, great strides have been taken in decreasing fossil-fuel dependence of electricity production with investments in wind- and solar harvesting technologies. However, the challenge of developing sustainable carbon-neutral fuels for transportation remains. One alternative that has received increasing attention in the last few years is the production of fuels using photosynthetic organisms such as microalgae or cyanobacteria. These organisms are capable of converting atmospheric carbon dioxide and water into useful hydrocarbons by harvesting solar energy (Parmar *et al*. 2011). These unicellular organisms hold the advantage over plant-based biofuels by being a non-feedstock resource, capable of utilizing non-arable land and having higher per-acre productivity (Johnson *et al*. 2018). Cyanobacteria, being prokaryotes, have the added benefit of being genetically tractable which gives researchers the option to increase productivity through metabolic engineering (Gao *et al*. 2016).

Isobutene and isoprene are small, volatile and highly reactive molecules used as a precursor to many different products such as rubbers, fuel additives and specialty chemicals (Rossoni *et al*. 2015, Lindberg *et al*. 2010). Using photosynthetic cyanobacteria, atmospheric CO_2 can be converted into isobutene or isoprene by genetically engineering certain metabolic pathways related to the Calvin-Benson-Bassham (CBB) cycle. These gas molecules can then be polymerised into longer hydrocarbons like jet fuel in a chemical reactor driven by solar energy. Jet fuel usually consists of aliphatic hydrocarbons with the lengths C8-C17 (Chou *et al*. 2002). This would provide the opportunity to produce well characterized, high performance jet fuel while greatly reducing the dependency of fossil fuel energy sources (Figure 1). A great advantage of bioproduction of these volatile hydrocarbons is that they are not retained in the cells or culture media. The gas is collected from the headspace of the cultivation vessel, circumventing costly and time-consuming downstream processing while also preventing premature cell death from toxic accumulations in the media. Isobutene and isoprene are currently almost exclusively extracted from fossil sources (van Leeuwen *et al*. 2012). There is a need to develop sustainable sources of these valuable products. For this work, the goal was to develop a putative pathway for isobutene production in cyanobacteria by introducing a heterologous metabolic pathway. The work also included constructing a photobioreactor (PBR) with a gas-trapping system to synthesise and harvest isoprene. Previously in the lab, working with isoprene had proven to be difficult due its volatile nature and its affinity to adhere to various materials. Because of this, appropriate materials had to be considered to both minimize isoprene absorption while also constructing a gas-tight system. The cyanobacterial strain used in this project is the glucose-tolerant *Synechocystis* sp. PCC 6803, further referred to as *Synechocystis*.

1.1 Aim

The work described in this report consists of two separate projects with the following goals:

- To introduce two heterologous enzymes in *Synechocystis* for the synthesis of intermediates necessary for isobutene production. To evaluate the isobutene synthesising capability of a Cytochrome P450 introduced in *Synechocystis*.
- To design and construct a photo-bioreactor and gas collection system capable of producing and harvesting isoprene directly from cyanobacteria. The work included identification of suitable materials and necessary components. This part of the work was done in collaboration with a group of chemists responsible for the design and construction of a photochemical reactor.

This thesis will contain two sections, one for each abovementioned aim which will be discussed separately.

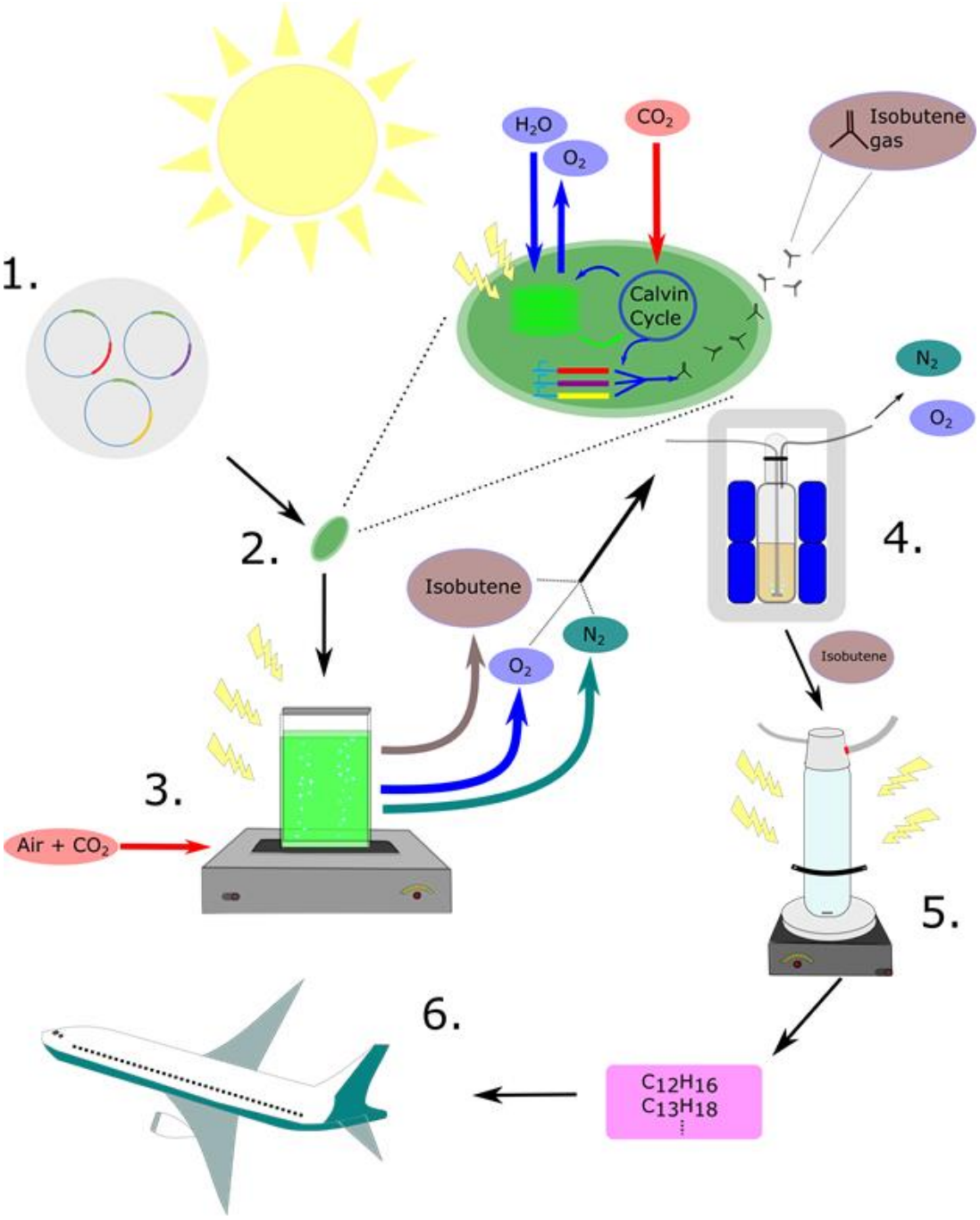

Figure 1: Overview production scheme and goals of the larger project as a whole. 1. Identify potential pathways of small hydrocarbon-production in microorganisms. 2. Insert said pathways in cyanobacteria that use sunlight as an energy source. 3. Grow the bacteria in photobioreactors. 4. Separate the biofuel precursors from other gaseous compounds. 5. Polymerize the small hydrocarbons into longer chains in photochemical reactors. 6. Scale-up production and release market competitive jet fuel for industrial use.

1.2 Project outline

1.2.1 The potential jet fuel precursors isobutene and isoprene

Isoprene is a 5-carbon volatile hydrocarbon (Figure 2) that is currently produced entirely from petrochemical sources. In industry, isoprene is extracted from complex mixtures of hydrocarbons obtained through steam cracking of petroleum (Gao *et al*. 2016). Isoprene has two double bonds, which makes the molecule very suitable for polymerization reactions (van Leeuwen *et al*. 2012). Isoprene is also known as a terpenoid, which is a group of compounds that are natively produced in cyanobacteria via the 2-C-methyl-D-erythritol 4-phosphate (MEP) pathway. Despite this, isoprene is not a natively produced terpenoid. Dimethylallyl diphosphate (DMAPP) and isopentenyl diphosphate (IPP) are the universal precursors for terpenoid production in all biological systems (Chaves *et al*. 2018). However, isoprene synthesis only requires the DMAPP reactant. Heterologous expression of isoprene synthases (IspS) along with metabolic engineering efforts to shift carbon flux towards DMAPP has led to recent increases in cyanobacterial isoprene production (Lindberg *et al*. 2010, Chaves *et al*. 2018). Yet, the production of isoprene in cyanobacteria is not currently commercially viable. There is a need for large-scale systems of isoprene generation and harvesting (Bentley and Melis 2012). The work in this project aimed to demonstrate the possibility of capturing volatile hydrocarbons directly from cyanobacteria. The main goals were to identify materials and parts appropriate for a photo-bioreactor and gas collection system and construct a prototype that was capable of harvesting isoprene for polymerisation. The isoprene producing strain used for this part of the work was the already available engineered *Synechocystis* strain 2MEP-IspS2. This strain expresses a codon-optimized version of the isoprene synthase gene from *Ipomoea batatas*. The strain also expresses codon-optimized genes that encode enzymes known to be bottlenecks in the terpenoid synthesis pathway; the deoxy-D-xylulose-5-phosphate synthase (DXS) gene from *Coleus forskohlii* and IPP: the DMAPP isomerase (IPI) gene from *Synechocystis* (Englund *et al.* 2018).

Isobutene is a 4-carbon volatile hydrocarbon (Figure 2) that is, like isoprene, mostly obtained from petrochemical sources. Just like for isoprene, the reactive double-bond of isobutene is what makes the molecule attractive to use in polymerisation reactions (van Leeuwen *et al*. 2012). There is one company, Global Bio-energies, that produces bio-isobutene from second-generation carbon sources such as wheat- or corn-derived glucose through fermentation. Their microbial platform of choice is a genetically modified *Escherichia coli*-strain protected by 32 patents (van Leeuwen *et al*. 2012). As of this work, there is no known commercial production of isobutene or isoprene via cyanobacteria.

1.2.2 Bio-synthesis of isobutene

There are currently three known intermediates for biosynthesis of isobutene: isobutanol, isovalerate and 3-hydroxyisovalerate, Wilson *et al*. (2018) and Rossoni *et al*. (2015) identified an ATP-dependant enzyme from the archaea *Picrophilus torridus* as mevalonate-3-kinase (M3K), which catalyses the phosphorylation of 3-hydroxyisovalerate to a compound that is unstable and undergoes spontaneous decarboxylation to form isobutene. Isobutene has also

been biosynthesized from the fungal cytochrome P450 native to *Cystobasidium minutum*, formerly known as *Rhodotorula Minuta* (Fukuda *et al*. 1994). The enzyme was shown to produce isobutene from the substrate isovalerate. To investigate the possibility of cyanobacterial isobutene production via this enzyme (further referred to as Cyt.P450cm), this work aimed to design an *in vivo* pathway as described in Figure 2. Ketoleucine is a downstream metabolite of pyruvate and is the first substrate in the heterologous pathway. Pyruvate is synthesised from glucose through glycolysis and is also a product of the CBB cycle (Liang *et al*. 2018). Cytochrome P450 enzymes are heme *b* containing monooxygenases that are often involved in complex and highly specific enzymatic reactions. In eukaryotes, they are membrane-bound proteins anchored in the endoplasmic reticulum (Wlodarczyk *et al*. 2016).

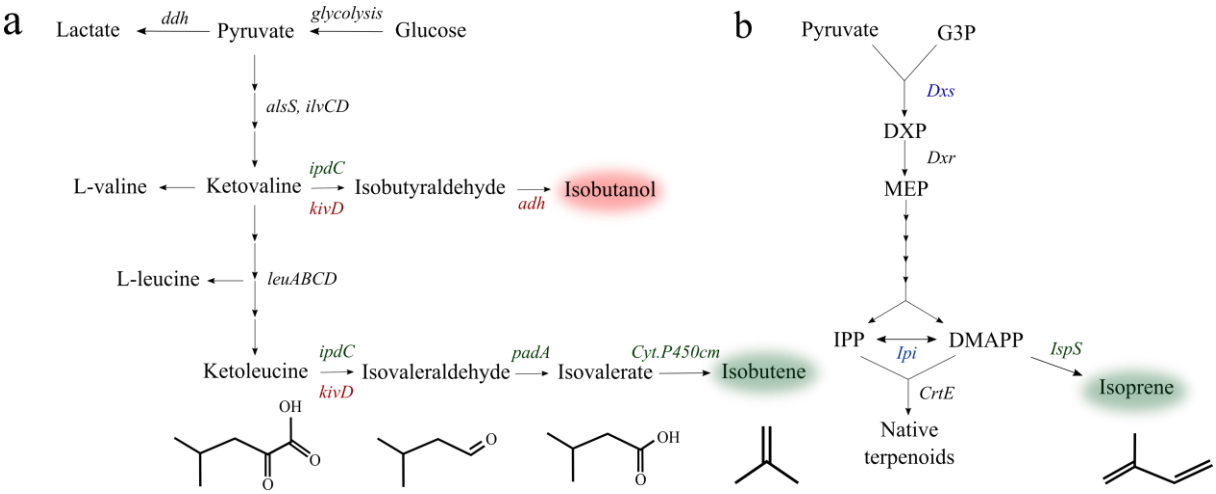

Figure 2: Simple overview of biosynthesis of isobutene and isoprene. (a) The putative biosynthetic pathway for possible isobutene production in *Synechocystis*. The substrate ketoleucine is a downstream product of ketovaline, a well-studied compound important in the biosynthesis of the bio-fuel isobutanol (Miao *et al*. 2017, 2018). The inserted genes are marked in green; *ipdC* from *Salmonella typhimurium, padA* from *E. coli* and Cyt.P450cm from *Cystobasidium minutum*. (b) Simplified overview of the MEP pathway in *Synechocystis* with heterologous introduction of IspS in the 2MEP-IspS2 strain marked in green. The codon-optimized genes *Dxs* and *Ipi* are marked in blue.

Wlodarczyk *et al*. (2016) introduced two membrane bound cytochrome P450s and a soluble glycosyltransferase from the plant *Sorghum Bicolor* in *Synechocystis* and observed expression of the cytochromes in the thylakoid membrane as well as active catalytic function. They showed that the cytochromes could be reduced by the native electron transport chain, photosystem I (PSI) and ferredoxin, enabling proper activity. If a similar approach can be taken with the isobutene-producing Cyt.P450cm from *Cystobasidium minutum* and facilitate production of isobutene in *Synechocystis*, a new pathway capable of providing solar driven biofuel precursors is open for future research and refinement.

For there to be an *in vivo* production of isobutene at all in *Synechocystis*, there needs to be access to substrate and substrate precursors for Cyt.P450cm. Xiong and coworkers highlighted two different enzymes capable of ketovaline- and ketoleucine degradation; α-ketoisovalerate decarboxylase (KivD) from *Lactococcus lactis* and indolepyruvate decarboxylase (IpdC) from *Salmonella typhimurium*, see Figure 2 (Xiong *et al*. 2012). These

carboxylases have differences in substrate affinity and catalytic rate, where IpdC has a higher K_{cat}/K_m ratio, also known as specificity constant, favoring the ketoleucine pathway (Xiong *et al*. 2012). The K_{cat}/K_m ratio of IpdC for ketoleucine was reported to be 22.2 $mM^{-1}s^{-1}$ as compared to 13.2 $mM^{-1}s^{-1}$ for KivD. In the same study an enzyme from *Escherichia coli*, phenylacetaldehyde dehydrogenase (PadA), was shown to catalyse isovaleraldehyde to isovalerate. This served as the basis for the decision to construct the *in vivo* isobutene pathway using IpdC and PadA as enzymes to increase the substrate availability for Cyt.P450cm.

2 Materials and methods

The materials and methods description below is divided into two segments; one for Cyt.P450cm and one for the IpdC and PadA proteins.

2.1 Cytochrome P450

2.1.1 Strain and cell cultivation

For analysis of Cyt.P450cm, a *Synechocystis* strain that had previously been conjugated with a pEEC-Cyt.P450cm plasmid, low copy plasmid with a chloramphenicol resistance cassette, was used. The Cyt.P450cm producing *Synechocystis* strain was grown in batch cultures in a total volume of 3.6 L in 20 mM HEPES-NaOH (pH 7.5) buffered BG-11 medium, stirred with sterile filtered air. An empty vector (EVC) control strain without gene of interest (GOI) or *ccdB* was also grown under identical conditions. The cultures were grown in continuous white light, 60 µmol m^{-2} s^{-1}, and at a temperature of 30 °C to cell densities of 0.6-1.3, OD750, before harvesting. The cells were harvested 7 days after inoculation of large-scale cultures by centrifugation in 50 ml falcon tubes (5000xg, 4°C, 15 min).

2.1.2 Thylakoid isolation

All steps in thylakoid isolation after cell disruption were performed in dim green light and at 4 °C or on ice. After centrifugation of the *Synechocystis* cultures, the pellets were washed with 5 ml washing buffer (50 mM HEPES-NaOH, pH 7.5, 20 mM $CaCl_2$, 10 mM $MgCl_2$) and spun down once more (5000xg, 4°C, 15 min). Pellets resuspended in 5 ml buffer (50 mM HEPES-NaOH, pH 7.5, 20 mM $CaCl_2$, 10 mM $MgCl_2$, 800 mM sorbitol) with added 100x ProteaseArrest ™ (G-Biosciences) and were aliquoted into two fractions. One cell fraction was disrupted though sonication, four times 15-second pulses, 20% of max amplitude. The other fraction was lysed using acid washed glass beads, in a bead beater (Precellys-24 homogenizer, Betin technologies) for three rounds of 30 seconds. The cells were kept on ice in between rounds. The cell debris was removed by centrifugation (1000xg, 4°C, 5 min) and the supernatant was centrifuged (18000xg, 4°C, 25 min) to pellet the thylakoid membranes. The supernatant, i.e. the soluble protein fraction, was collected and stored at -80°C. All supernatant from the remaining thylakoid pellet was removed and the pellet was resuspended

in storage buffer (50 mM HEPES-NaOH, pH 7.5, 20 mM CaCl2, 10 mM MgCl2, 600 mM sucrose, 1 M glycine betaine).

2.1.3 Chlorophyll *a* estimation

The chlorophyll *a* concentration was estimated by mixing 20 µl concentrated thylakoids with 80 µl storage buffer in 1 ml cuvettes and adding 900 µl 100% methanol. After 10 min of incubation at room temperature, OD665 was measured using a spectrophotometer. The chlorophyll *a* concentration was calculated using the following formula: OD665 value x 50 (dilution factor) x 12.7 (extinction coefficient, Meeks and Castenholz, 1971) = µg Chl *a* / ml. The thylakoid membrane fractions were aliquoted for oxygen evolution experiments and were flash frozen with liquid nitrogen and stored at -80°C.

2.1.4 SDS-Page and Western blot analysis

Thylakoid samples equivalent of 3.2 µg Chl *a* were mixed with 4x Laemmli buffer and boiled at 95°C for 5 min. The samples were then administered to TGX mini-gels (BioRad, US) and run in Tris running buffer, at 200 V for 30 min. The gel was transferred onto a blot transfer membrane using the Trans-Blot Turbo transfer system (Bio-Rad, US) and was blocked in 5% (w/v) milk in room temperature overnight. The membrane was washed twice with TTBS (Tris buffered saline with Tween) for 5 min then 15 ml of Strep II antibody (Abcam, 1:1000 dilution in TTBS) was added. The membrane was incubated on shaker for one hour at room temperature then washed 4x5 min in TTBS. Additionally, the membrane was incubated with 15 ml anti-rabbit antibody (1:10 000 dilution in TTBS) for 1 hour 15 min, shaker, room temperature then washed with TTBS 3x5 min. The horseradish peroxidase (HRP) -conjugated secondary antibody was detected using Clarity western substrate reagents. The membrane was imaged using the ChemiDoc XRS+ system (BioRad, US).

2.1.5 O_2 evolution

Oxygen evolution of photosystem II (PSII) was measured using a Clark-type oxygen electrode (Hansatech, King's Lynn, UK) at 25 °C. A slide projector with a 590 nm cut-off filter was used to provide saturating light. The electrode was calibrated by first filling the chamber with water and set stirring with a magnet. After 30 min the water was air-saturated and the dissolved O_2 concentration was set as the max value. The chamber was then flushed with nitrogen gas until the dissolved O_2 level reached its lowest concentration, this was set as the baseline. Oxygen evolution of the thylakoid membranes was measured with protein corresponding to 5 µl Chl *a*/ml with 1 mM phenyl-p-benzoquinone (PBQ) as electron acceptor. The electrode chamber was filled to 1 ml with TSCB buffer (50 mM HEPES-NaOH pH 7.5, 200 mM sucrose, 20 mM $CaCl_2$, 10 mM $MgCl_2$). Measurements were taken under continuous stirring and the chamber was washed with deionized water in between runs.

2.1.6 Isobutene production assay

Thylakoids preparations (protein amount corresponding to 25 µg Chl *a* from the sonicated fractions) were mixed with 0.01 mM spinach ferredoxin, 0.1% (w/v) Dodecyl β-D-maltoside (β-DM), 22.5 µM equine cytochrome c, 1 mM dithiothreitol (DTT), 3.6 mM sodium

ascorbate, 0.11 mM 2,6-dichlorophenolindophenol (DCPIP), 50 mM isovalerate in gas-tight GC vials and 20 mM HEPES, pH 7.5, to a final reaction volume of 100 µl. The vials were incubated at 30°C on a shaker under 80 µmol m^{-2} s^{-1} continuous white light. The gas phase was measured using GC with a packed column and FID (Perkin-Elmer, Waltham, MA, USA).

2.2 Indolepyruvate decarboxylase and phenylacetaldehyde dehydrogenase

2.2.1 Gene synthesis and construct design

The genes coding for a phenylacetaldehyde dehydrogenase (PadA, accession number P80668*)* from *Escherischia coli,* and indolepyruvate decarboxylase (IpdC, accession number E8XF61*)* from *Salmonella typhimurium*, were optimized to the codon usage that is preferred in *Synechocystis* using the GeneDesigner 2.0 software. The optimization included a cutoff frequency of 12% to exclude codons that are very rarely present in *Synechocystis*. The DNA sequences were synthesized by GenScript (Piscataway, NJ, USA), cloned in a *pUC-57* vector. For the cloning of the genes *padA* and *ipdC*, the low copy plasmid pEEK2 (Miao *et al*. 2017) containing a Bi-cistronic design element (BCD, Mutalik *et al*. 2013), a kanamycin resistance cassette and the strong Ptrc promoter was used as vector. pEEK2 contains a broad host replication origin RSF1010 allowing expression both in *E. coli* and *Synechosystis* 6803. The strong Ptrc promoter is inducible in *E. coli* but constitutive in *Synechocystis* (Englund 2016). The SnapGene software was used to visualise the bioinformatic work.

2.2.2 Cloning of *ipdC* and *padA* in *E. coli*

The pUC-57 vectors containing the *padA* and *ipdC* genes were transformed into competent *E. coli*, strain DH5a-Z1. This was done by adding 10 ng of plasmids to melted stocks of competent DH5a-Z1 cells which were then incubated for 20 min on ice followed by 45 seconds of heat-shock treatment at 42 °C. The cells were subsequently incubated on ice for 5 more min and lastly 1 ml of LB was added to the cells which were incubated at 37°C for 1.5 hours. 100 µl of each culture was plated on LB agar plates supplemented with 100 µg/ml ampicillin. However, pEEK2 transformants were plated on 50 µg/ml kanamycin plates.

Overnight cultures of positive transformants were grown in 6 ml LB supplemented with the appropriate antibiotic at 37 °C. Plasmid preparations were performed on overnight cultures of *E. coli* using the GeneJET Plasmid Miniprep Kit (Thermo Scientific) according to the manual provided by the manufacturer. DNA concentrations were measured using a Thermo scientific nano-drop 2000 UV-visible spectrometer. Digestions of plasmids were done using the Thermo Scientific Fast Digest enzymes according to the manual of the manufacturer with the exception of the addition of FastAP alkaline Phosphatase to the pEEK2 digests to prevent re-ligation. The digests were purified using Zymo Research DNA clean and Concentrator Kit according the manufacturers manual. The purified digestions of *ipdC*, *padA* and *pEEK2* were then ligated to form the pEEK2-IpdC and pEEK2-PadA constructs. The ligations were performed using Biolabs QuickLigase according to the manual provided by the manufacturer. Transformation of these constructs were performed as described earlier in this section.

Plasmid preparations were performed on positive colonies and their plasmids were mixed with appropriate primers (Table S1) and sent to Eurofin Genomics for Sanger sequencing. Confirmation of the genetic inserts was also confirmed using colony PCR according to Table S3 with appropriate primers (Table S1).

2.2.3 Protein expression in *E. coli*

25 ml of *E. coli* cultures were prepared in LB supplemented with 5.5% sterile filtered glucose in 100 ml E-flasks and were incubated at 37 °C under shaking for 2 h 15 min. IPTG was added to a final concentration of 1 mM and the cultures were incubated under the same conditions for 4 h. OD600 samples were taken before and after induction. The cultures were washed with 25 ml TBS, pH 8.0, and 150 µl ProteaseArrest^{TM} was added along with Lysozyme to a final concentration of 0.7 mg/ml. The cultures were sonicated for 5 cycles, 15 sec pulses, 40% max amplitude. The lysates were centrifuged at 5000xg/10 min/4°C and the supernatant was completely removed from the pellet which was resuspended in 25 ml TBS. Supernatant, membrane, as well as before and after induction samples were analysed using SDS-PAGE and western blot according to section 3.1.4.

2.2.4 Conjugation of *ipdC* and *padA* into *Synechocystis*

Synechocystis WT was grown at 30°C under 40 µmol m^{-2} s^{-1} white light illumination to an OD750 of about 1.5. 3 ml of overnight cultures of *ipdC* and *padA E. coli* mutants were grown as well as a 6 ml culture of *E. coli* HB101 helper strain carrying the plasmid pRL443-Amp^{R}. pRL443. The cargo and helper strains were washed twice with fresh LB without antibiotics and then mixed together. The mixed cultures were centrifuged and the pellet resuspended in 200 µl LB. 20 µl of *Synechocystis* WT was added to each mixture which were then incubated at 30 °C under 40 µmol m^{-2} s^{-1} white light for 1.5 hours. After incubation, 100 µl of each mixture was plated on nitrocellulose filters on BG-11 plates without antibiotics. The plates were placed in low light for one day after which the filters were transferred to BG-11 plates containing kanamycin. The plates were placed in high light for approximately three weeks.

The genetic inserts in *Synechocystis* was also confirmed using colony PCR according to Table S3 with backbone and gene-specific primers (Table S1).

2.2.5 Cell cultivation and crude cell extract preparation

Synechocystis mutants harbouring the pEEK2-IpdC and pEEK2-PadA constructs were grown in 20 mL BG-11 supplemented with 50 mM HEPES, pH 7.5, 50 mM $NaHCO_3$ and 50 µg/mL kanamycin at 30 °C under 40 µmol m^{-2} s^{-1} white light illumination. Crude cell extracts of *Synechocystis* mutants were prepared by using the following protocol:

1. Harvest cells through centrifugation, 8000xg/5 min/4°C
2. Wash the pellet with 200 µl BG-11
3. Spin down, 8000xg/2 min/4°C
4. Add acid washed glass beads (425-600 µm diameter)
5. Add 200 µl of protein extraction buffer

a. Add 2 µl of ProteaseArrest™
6. Disrupt the cells using the Precellys-24 homogenizer, 3x30 sec with 2 min on ice between rounds. All following steps were done in dim green light and at 4 °C.
7. Centrifuge 1000xg/5 min/4°C and collect the supernatant
8. Repeat the centrifugation and collect the supernatant

The protein extraction buffer used for pEEK2-IpdC was PBS (136 mM NaCl, 2.6 mM KCl, 10 mM Na_2HPO_4, 1.76 mM KH_2PO_4) supplemented with 5 mM $MgCl_2$ and 0.1 mM TPP (thiamine pyrophosphate) pH 6.5. PBS pH 7.3 was used for pEEK2-PadA. Total protein content of the crude cell extracts was measured using BioRad DC Protein assay according to the manual provided by the manufacturer.

2.2.6 Crude cell extract activity assay

Crude extract enzyme assays were prepared in small GC-vials with PTFE membrane using crude cell extracts of pEEK2-PadA, pEEK2-IpdC and pEEK2 mutants. Each reaction contained 50-100 mg/ml protein, 1 µl of the appropriate substrate and added PBS buffer up to a total reaction volume of 100 µl. In the vials containing PadA protein NAD+ was added to a final concentration of 750 µM. The enzyme assays were performed in darkness at 30°C for 16 hours then placed in 60°C for 5 hours. The gas phase of the GC-vials was measured in GC using an extended program to increase resolution, 15 min, 6ml/min of nitrogen as carrier gas, oven temperature 200°C. The peak areas obtained were compared to substrate standards that had undergone similar heat treatment to produce characteristic degradation products.

2.2.7 Western blot of IpdC and PadA

Western blots of prepared crude extracts corresponding to 50 µg were performed as according to section 3.3.3. The membrane was stained using Thermo Scientific PageBlue™ staining solution according to the manual provided by the manufacturer.

2.2.8 Substrate standard curves

Dilution series of ketoleucine, isovalerate and isovaleraldehyde were prepared in dichloromethane (DCM) and run in capillary GC (ELITE-WAX) to obtain standard curves for said substrates. Similar dilution series were also prepared in acetonitrile and analysed using liquid chromatography coupled with a mass spectrophotometer (LC-MS).

3 Results

3.1 Cytochrome P450 in *Synechocystis*

3.1.1 Western blot of Cyt.P450cm

As an initial analysis to determine whether the Cyt.P450 protein was successfully integrated into the thylakoid membrane of *Synechocystis*, SDS-PAGE and western blot was performed on thylakoid preparations (Figure 3). It is apparent that Cyt.P450 is expressed in *Synechocystis* and that the protein is positioned in the thylakoid membrane. The bead beat fractions seems to have a higher protein concentration when comparing to the sonicated fractions. This is supported by the strong bands shown in the western blot and the loading control. In order to verify the viability of the prepared thylakoid membranes, oxygen evolution experiments were performed.

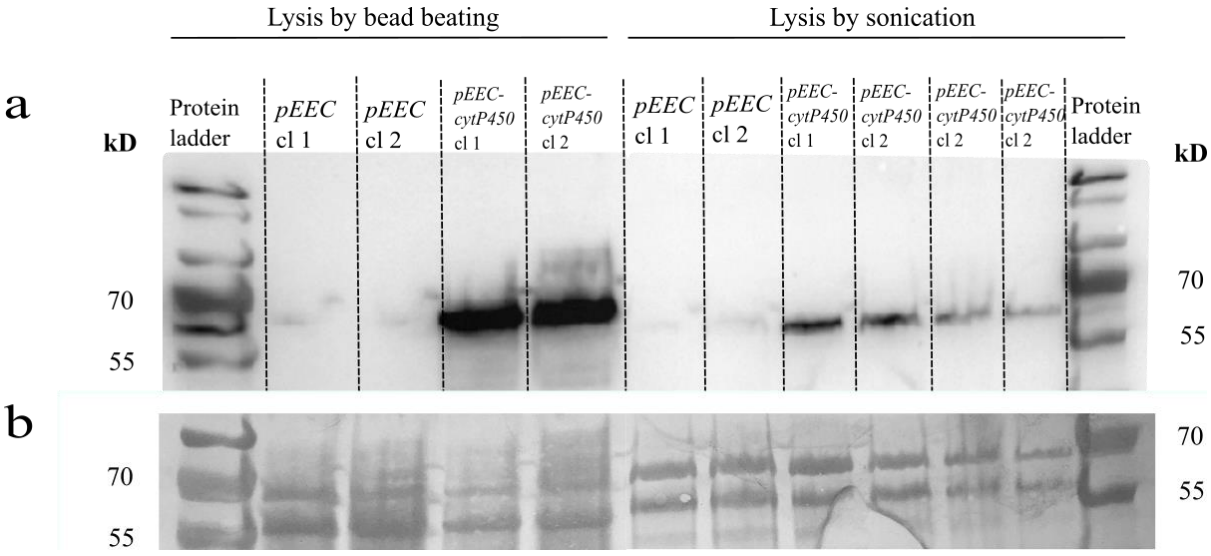

Figure 3: Western blots of isolated thylakoid membranes obtained through two methods of cell lysis from *Synechocystis* containing the pEEC-Cyt.P450cm insert. (a) Two empty vector- (EVC) and two Cyt.P450cm clones were loaded with protein corresponding to 3.2 µg of Chl *a*. The second clone of sonicated Cyt.P450 was also diluted to 1.6 and 0.8 µg of Chl *a*. The expected protein size of Cyt.P450cm is 60 kD. (b) Stained western blot membrane used as loading control.

3.1.2 Oxygen evolution of thylakoid membranes

As depicted in Figure 4, the oxygen evolution of the thylakoid membrane preparations was comparable to the ones in intact WT *Synechocystis* cells. Most importantly, there is no major difference between the control (pEEC) and the Cyt.P450cm mutant. This suggests that the integration of the thylakoid membrane-bound protein have had no negative effect on the photosynthetic efficiency of the mutant. Interestingly, a sharp difference in activity between the sonicated and bead-beat fractions was observed, indicating that the method of lysis could have an impact on the quality of the thylakoid membranes. However, to confirm these theories more replicates need to be included in order to provide statistical significance. The

added $NaHCO_3$ to the WT cells increases activity 4-fold through the addition of an electron sink. This properly highlights carbon-fixation as the rate-limiting step of photosynthesis.

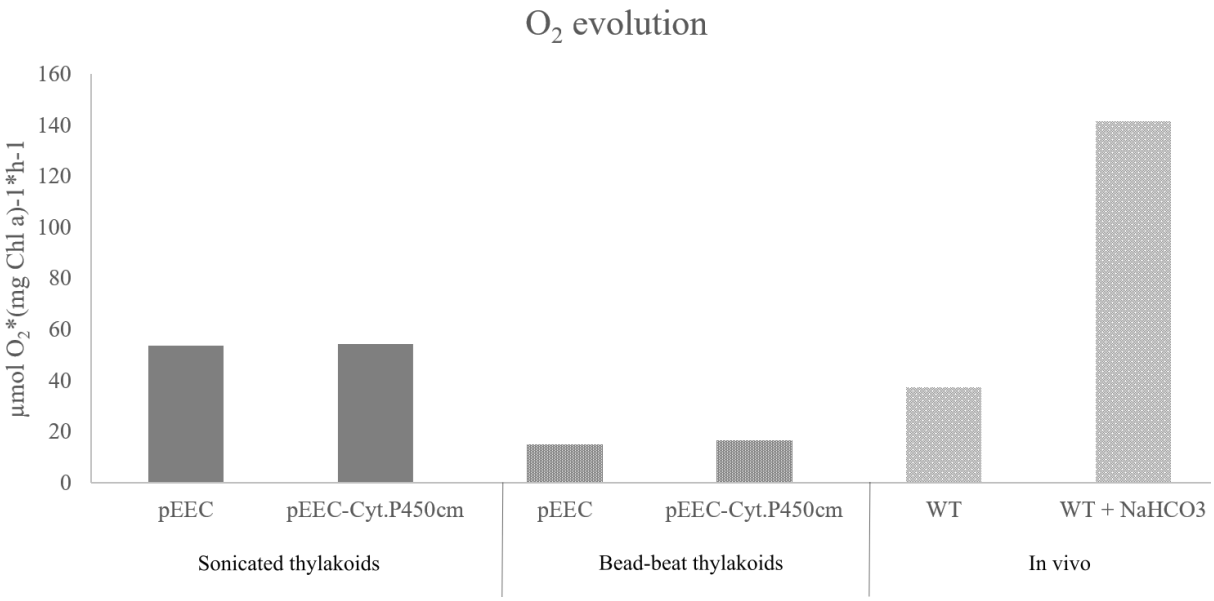

Figure 4: Oxygen evolution of isolated thylakoid membranes and whole WT *Synechocystis* cells. Oxygen evolution of PSII from isolated thylakoids was analysed using PBQ as electron acceptor (PSII→PBQ). Whole-chain photosynthetic oxygen evolution rate evaluated using intact WT *Synechocystis* cells (PSII→PSI→CBB/$NaHCO_3$).

3.1.3 Isobutene production assay with Cyt.P450cm

Continuing, the putative isobutene production capability of Cyt.P450cm was evaluated using an *in vitro* enzyme assay where the gaseous products were analysed using GC (Figure 5). The motivation for this approach was that the activity of Cyt.P450cm had previously been evaluated in the lab using whole cells and adding isovalerate. No difference was observed between EVC and Cyt.P450cm expressing strains. It was then not clear whether the isovalerate failed to enter the cells or if the protein was inactive. The effort was then made to perform the activity assay on isolated thylakoid membranes. After a 15-hour reaction, the amount of isobutene obtained from the pEEC-Cyt.P450cm strain was the same as from the pEEC control (Figure 5). These results suggest that even though the Cyt.P450 protein seems to have been successfully inserted into the thylakoid membrane, it is not producing isobutene or at least not a noticeable amount. Thylakoid isolation and the activity assay were repeated using a higher concentration of ferredoxin (Figure S1). The results from this assay were very similar to the first. The isobutene concentrations from pEEC-Cyt.P450cm and pEEC thylakoids are essentially the same. The presence of isobutene in both pEEC-Cyt.P450cm and pEEC reactions indicates that the putative substrate for Cyt.P450, isovalerate, spontaneously decomposes into isobutene or a very similar compound such as isobutane. This vastly complicates the matter of evaluating the isobutene production of the protein.

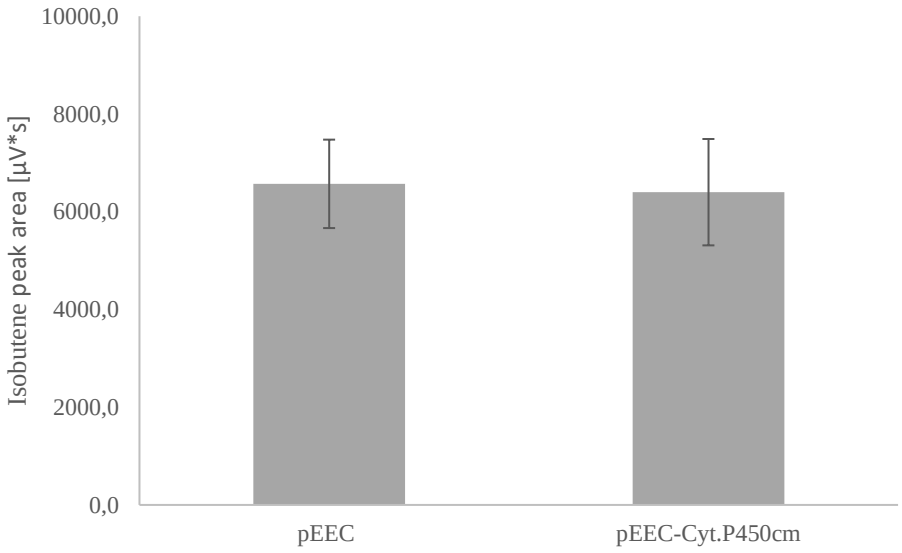

Figure 5: Activity of Cyt.P450cm investigated through *in vitro* enzyme assay. Protein obtained through thylakoid membrane isolation. Contents of each reaction: protein from thylakoid preparations corresponding to 25 µg Chl *a*, 0.01 mM spinach ferredoxin, 0.1% (w/v) Dodecyl β-D-maltoside (β-DM), 22.5 µM equine cytochrome c, 1 mM dithiothreitol (DTT), 3.6 mM sodium ascorbate, 0.11 mM 2,6-dichlorophenolindophenol (DCPIP), 50 mM isovalerate and 20 mM HEPES, pH 7.5 to a final reaction volume of 100 µl. The retention time of the supposed isobutene peak matched the retention time of an isobutene standard. Incubation time 15 h at 30 °C.

3.1.4 Spontaneous decomposition of isovalerate

Given the fact that spontaneous decomposition of isovalerate, the putative substrate of Cyt.P450cm, could be observed in the *in vitro* isobutene assays, an isovalerate decomposition rate assay was performed (Figure 6). The assay was performed using GC-vials at 30°C with a total reaction volume of 100 µl. Three different solvents were used; (i) BG-11 supplemented with 50 mM HEPES, pH 7.5, (ii) dH_2O supplemented with 50 mM HEPES, pH 7.5 and (iii) dH_2O with a pH of 5. Isovalerate was added to each vial to a final concentration of 1%. It is clear that the rate of isovalerate decomposition is greatly reduced in these solvents as compared to in the thylakoid preparations (Figure 5 and Figure S1). An approximation can be made by comparing the isovalerate concentration, incubation time and isobutene peak area of Figures 6 and S1 that the rate of decomposition of isovalerate in BG-11 is about 600 times slower than in thylakoid preparations of *Synechocystis*. Additionally, the addition of ferredoxin and cytochrome C seems to facilitate the decomposition of isovalerate to isobutene.

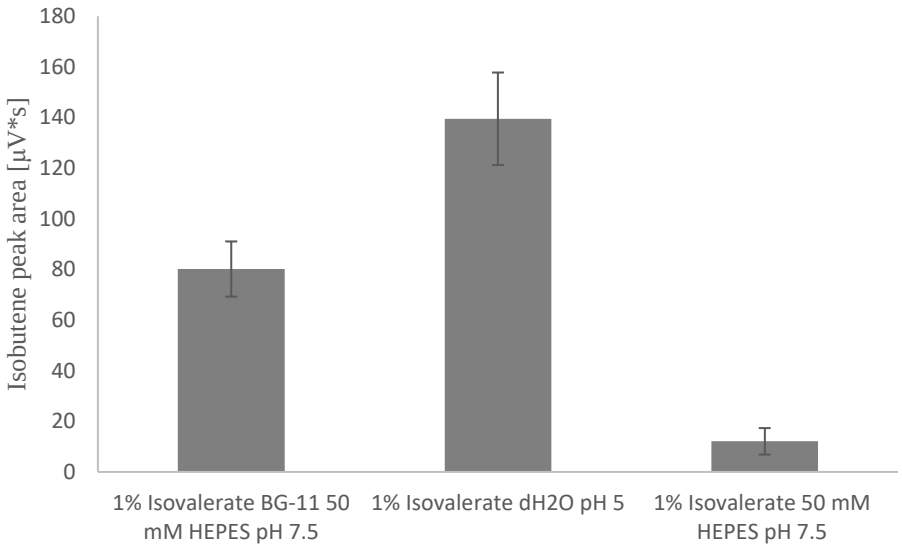

Figure 6: Isovalerate decomposition in different solvents. Total reaction volume 100 µl. Five-day incubation at 30 °C under shaking. 1% isovalerate corresponds to 100 mM.

3.2 Indolepyruvate decarboxylase and phenylacetaldehyde dehydrogenase

3.2.1 Isovaleraldehyde and isovalerate quantification

In order to be able to quantify any production of the proteins IdpC and PadA, standards of isovaleraldehyde and isovalerate were done using both capillary GC and LC-MS. However, no reliable standard curves of isovalerate or isovaleraldehyde could be obtained using capillary GC or LC-MS (data not shown).

3.2.2 Cloning of *ipdC* and *padA* in *E. coli*

The transformation of pEEK2-IpdC and pEEK2-PadA constructs in DH5a-Z1 yielded nine and seven colonies, respectively. Three colonies of each construct were analysed using colony PCR (Figure 7) using appropriate primers (Table S1). DNA from the colonies that displayed correct fragment size was sent for Sanger sequencing which confirmed the presence of the constructs (data not shown).

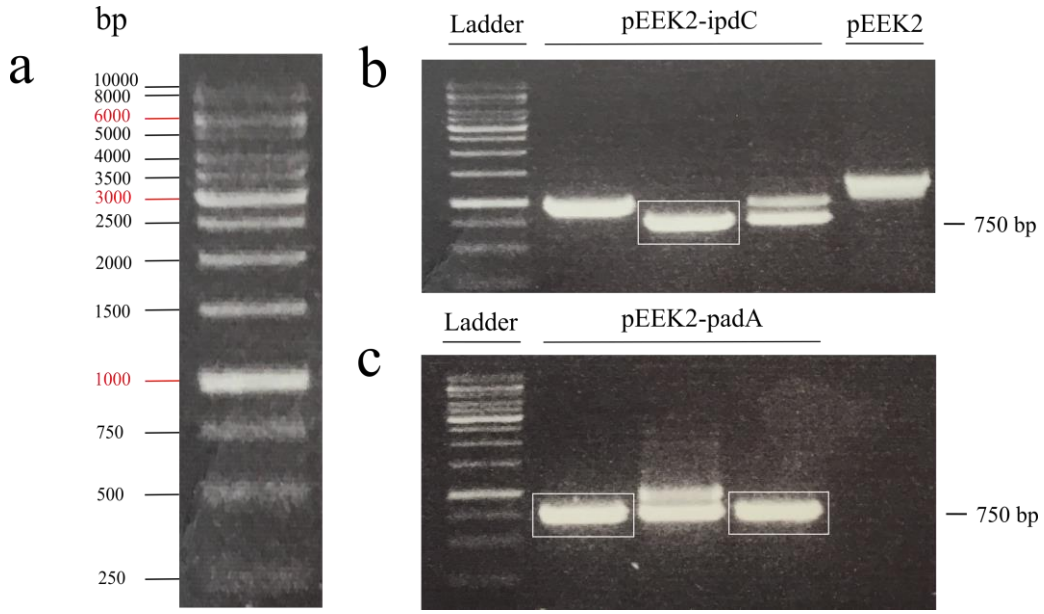

Figure 7: Colony PCR of transformed *E. coli*. DNA ladder (a). Colonies of pEEK2-IpdC (b) Colonies of pEEK2-PadA (c) The white boxes show the bands with the expected fragment lengths. Minipreps of pEEK2-plasmids were used as positive control. The fragment lengths of both pEEK2-IpdC and pEEK2-PadA were expected to be 750 bp.

Western blots of induced *E. coli* containing the genetic inserts show that there is clear overexpression of the Strep II-tagged proteins (Figure 8). There are visible bands for the non-induced *E. coli* samples as well, indicating a leaky promoter. The size of IpdC corresponds to the expected molecular weight of 60 kD. However, the protein size of PadA seems to be larger than expected. The expected protein size of PadA without Strep II tag is 53.7 kD but the protein size that can be approximated from the western blot appears to be over 60 kD. The molecular weight of the Strep II tag is 1 kD. Similar results are depicted in Figure 9. To determine where in the cells the IpdC and PadA proteins were located, the membrane and soluble fractions of *E. coli* lysates were analysed with a western blot (Figure 9). In this western blot the proteins appear to be soluble which was to be expected. There are strong bands in the membrane fractions as well, this could possibly be due to protein aggregations in inclusion bodies caused by high protein expression (Singh *et al*. 2015).

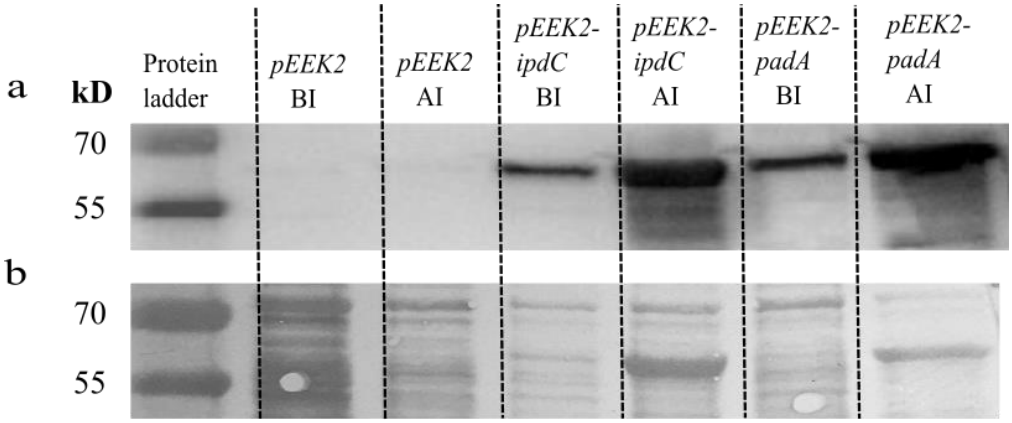

Figure 8: Western blot of PadA- and IpdC-producing *E. coli* strains. (a) *E. coli* lysates before induction (BI) and after induction (AI). (b) Stained western blot membrane used as loading control. The expected protein sizes of IpdC and PadA are 60 kD and 53.7 kD respectively. *E. coli* containing pEEK2 plasmid without *ccdB* used as negative control.

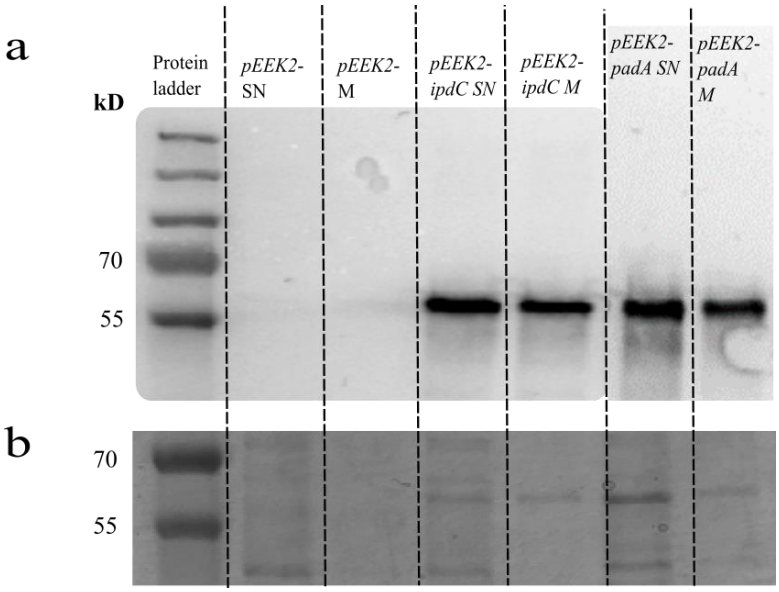

Figure 9: Western blot of *E. coli* with pEEK-IpdC and pEEK2-PadA inserts. (a) Supernatant (SN) and membrane (M) fractions of induced *E. coli* strains. (b) Stained SDS-PAGE gel for loading control. *E. coli* containing pEEK2 plasmid without *ccdB* used as negative control.

The presence of the genetic inserts in *Synechocystis* conjugants could be confirmed using colony PCR with gene-specific primers (Figure 10). The expected fragment sizes for IpdC and PadA were 950 and 200 bp respectively. Western blots of conjugants also show that there is protein expression of IpdC and PadA (Figure 11). This western blot was not normalized to OD or protein concentration but merely done to determine if the proteins were being expressed.

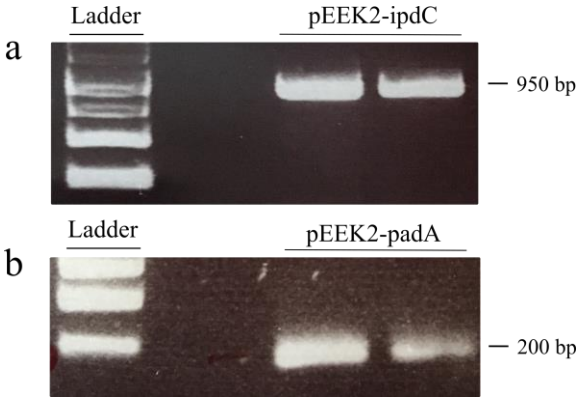

Figure 10: Colony PCR of colonies from conjugated *Synechocystis*. (a) pEEK2-IpdC colonies. (b) pEEK2-PadA colonies. Gene-specific primers for both pEEK2-IpdC and pEEK2-PadA were used.

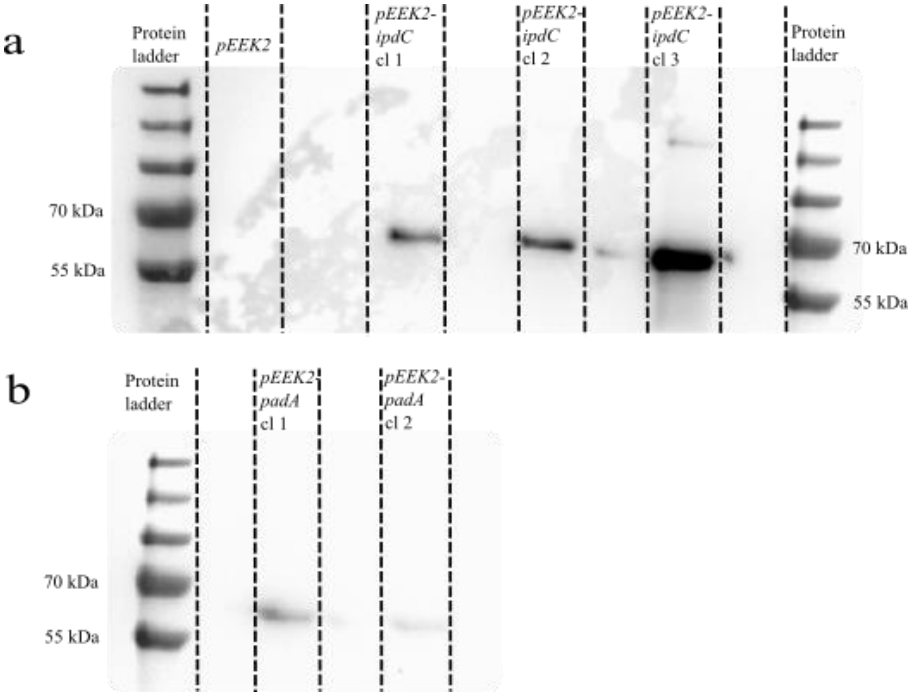

Figure 11: Western blot of *Synechocystis* mutants. (a) pEEK2-IpdC clones with pEEK2 EVC control, (b) pEEK2-PadA clones. Samples taken from 20 ml *Synechocystis* cultures, one pEEK2-PadA culture did not grow and is therefore not represented in the western blot.

3.2.3 Crude cell extract activity assay

In an attempt to identify produced isovaleraldehyde from IpdC and isovalerate from PadA, a crude extract enzymatic *in vitro* assay was performed. After the reactions all samples were heated in order to facilitate spontaneous decomposition of produced compounds. The headspace of the samples was analysed using a GC program designed to give high resolution of smaller gases. The intent was to create a fingerprint of substrate and product decomposition compounds that could be compared to crude extract controls (Figure 12).

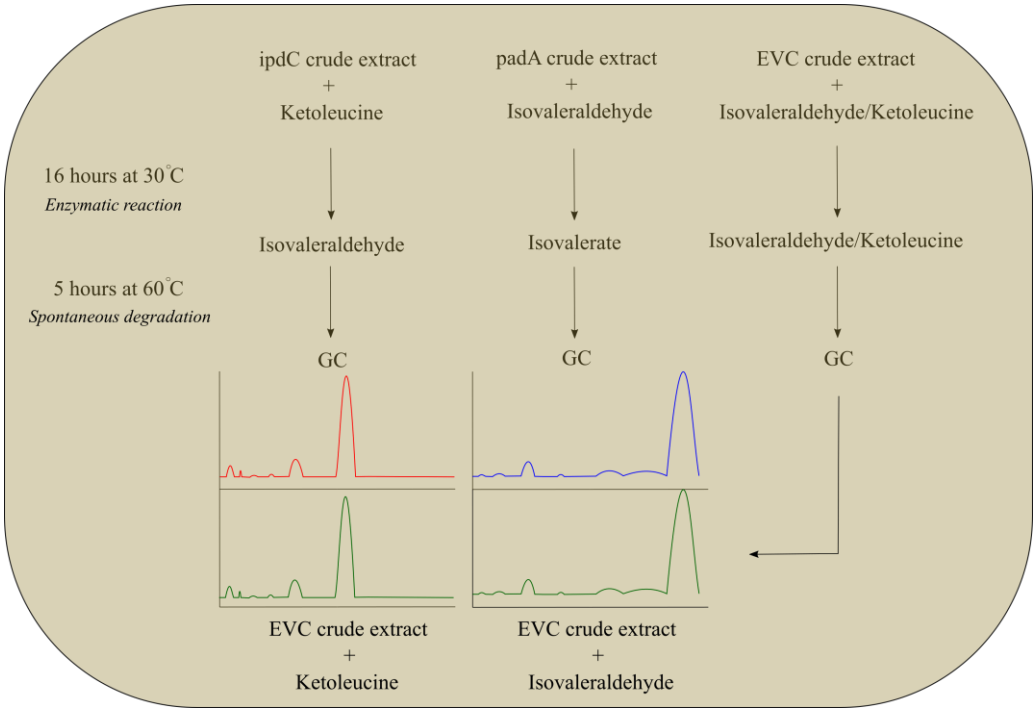

Figure 12: Strategy applied to detect products from crude extract activity assay of IpdC and PadA. The assay of crude extract was performed for 16 hours at 30 °C and were subsequently heat-treated for 5 hours at 60 °C. The headspace of each sample was analysed using GC and the resulting chromatograms compared to the ones of empty vector (EVC) crude extracts. The EVC crude extracts were submitted to the same conditions with either added ketoleucine or isovaleraldehyde. The GC chromatograms depicted in the figure are graphical representations.

All the peaks that were detected from heated samples were also detected from the crude extract controls. Meaning, no unique decomposition products that could indicate production of either isovaleraldehyde from IpdC, or isovalerate from PadA was detected. A sample of pure isobutene was run on the same GC program. Peaks near the same retention time were detected for the PadA crude extracts, indicating isovalerate production. However, a peak of similar size was also detected for the EVC crude extract with added isovaleraldehyde.

The *Synechocystis* clones used for the *in vitro* activity assay were two clones that had protein expression as seen in Figure 6. In order to verify potential protein activity a western blot of the same clones was prepared (Figure 13). However, in this western blot, no expression of IpdC was visible.

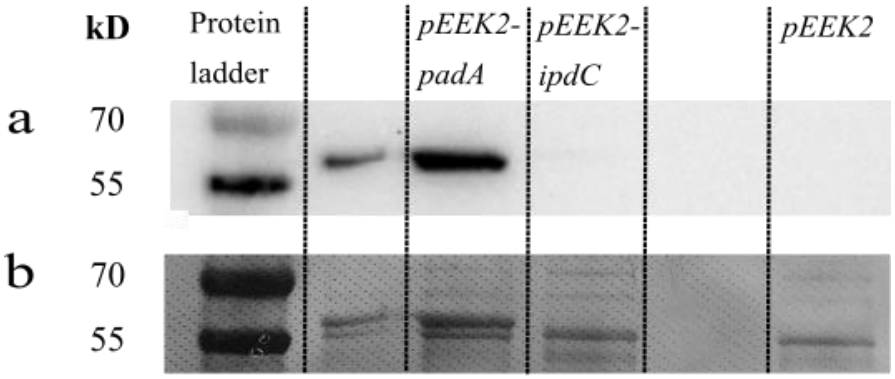

Figure 13: Western blot of *Synechocystis* mutants used in the *in vitro* activity assay. (a) Strep II-tagged protein blotted on membrane. (b) Stained membrane used as loading control. A total of 50 µg of protein was loaded in well 2, 3 and 5. The protein in the first well is overflow from the second well.

3.3 Photobioreactor and gas-trap system

The aim for this section of the thesis was the development of a photobioreactor and harvesting systems of isoprene and thus the methodology applied is merged with the results.

3.3.1 Materials for photobioreactor/gas-trap systems

In order to evaluate appropriate materials for the construction of a PBR and isoprene harvesting system, the isoprene resistance properties of some common laboratory materials were examined. Samples of silicone, polyvinylidene fluoride (PVDF) and nylon were submerged in isoprene for 18 days and their relative increase in mass was recorded (Figure 14).

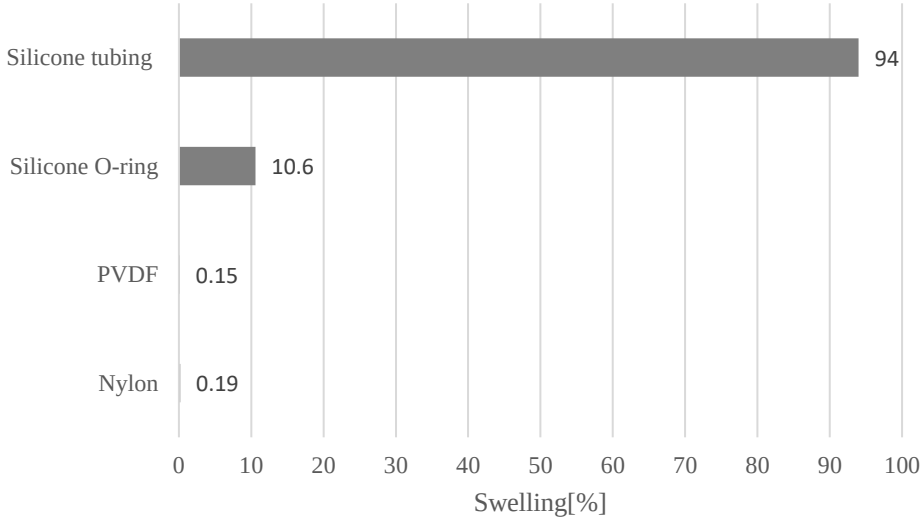

Figure 14: Isoprene absorption of different polymers. X-axis represents relative increase in mass (swelling). Samples of materials were submerged in isoprene for 18 days and the relative increase in mass was recorded. PVDF and nylon are common materials for connections of tubing like Luer fittings and reduction fittings.

Both PVDF and nylon showed good chemical resistance towards isoprene, therefore we decided to use these materials for fittings and connections for the PBR and the harvesting system. Polytetrafluoroethylene (PTFE), a material similar to PVDF in its structure, was chosen as the material for longer tubing. The backbone of the PTFE polymer is fully fluorinated which offers greater chemical resistance than PVDF, which is semi-fluorinated (Zhang *et al*. 2017). The usage of silicone was kept to a minimum due to its absorbing properties. Any silicone tubing used in the system was wrapped in PTFE tape in an attempt to decrease losses.

In order to observe the rate of diffusion of isoprene through silicone, a scaled-down (135 ml) version of a PBR was constructed. The reactor had a Hamilton PTFE membrane for isoprene sampling, one tube for gas inflow and one for outflow. The amount of silicone tubing was kept to a minimum and wrapped in PTFE tape to evaluate the lowest possible isoprene leakage of the PBR. 1 µl of isoprene was placed in the reactor which was then sealed. Isoprene samples were taken from the PBR and run in GC over the course of three days (Figure 15). Initially, the rate of isoprene diffusion was rapid and then slowly decreased over time.

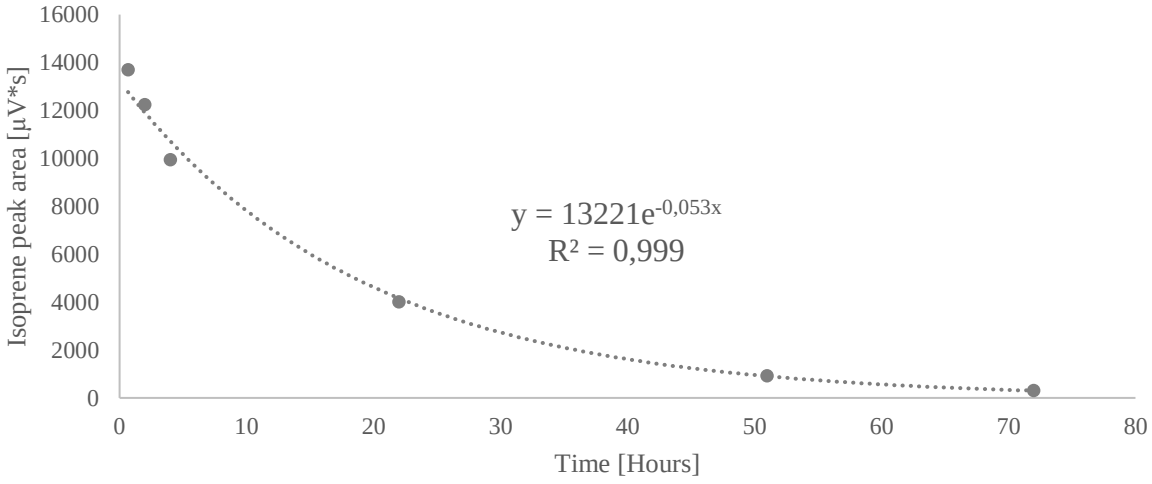

Figure 15: Diffusion of isoprene though silicone tubing by measuring concentration of isoprene gas in scaled-down PBR. Data fitted with an exponential trendline.

3.3.2 Continuous gas trap system

Two main types of PBR/gas-trap systems were evaluated, continuous and intermittently flushed gas trap systems. Initially, cultivation and harvesting of isoprene produced by *Synechocystis* was evaluated using a continuous system. Effluent gasses of cultures were led through the alkane dodecane to facilitate isoprene retention.

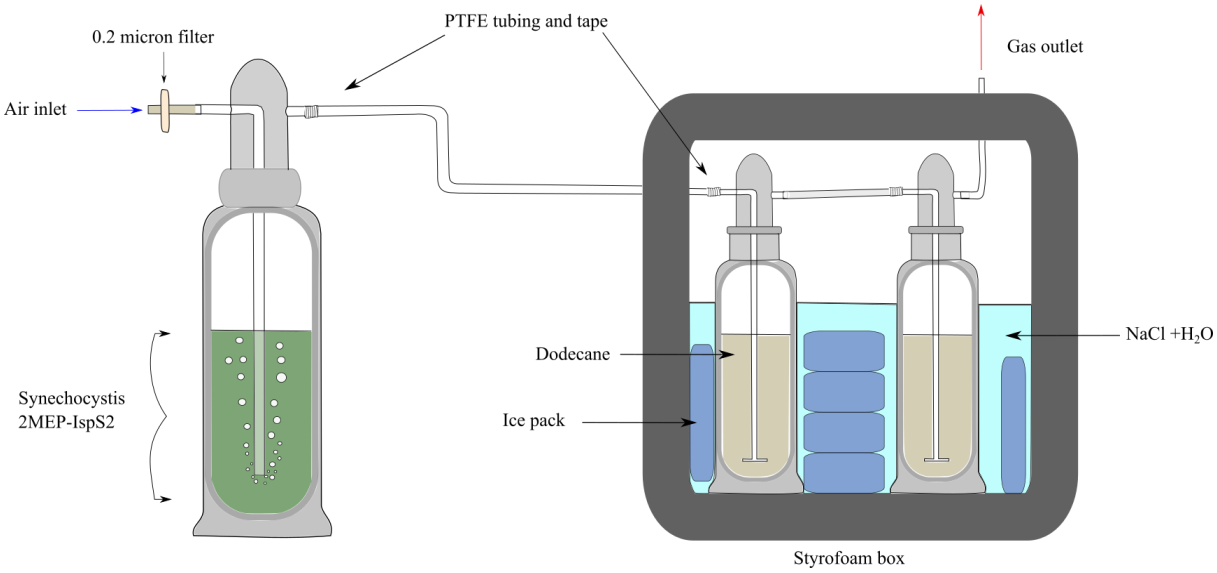

Figure 16: Schematic of continuous PBR/cold-trap system. Culture of 2MEP-IspS2 and pEEC control *Synechocystis* strains grown in 500 ml bubbling flasks at 30°C, under aeration and 60 µmol m^{-2} s^{-1} continuous white light. Two bubbling flasks containing dodecane connected in series with PTFE tubing acts as the isoprene trap. Dodecane chilled by ice water supplemented with NaCl.

Two gas traps were constructed (Figure 16) using water-tight boxes filled with 4 L of chilled saltwater with a freezing point of -9°C and two 250 ml bubbling flasks filled with 50 ml dodecane connected with PTFE tubing. The boiling point of isoprene is 34°C and the purpose of the chilled dodecane was to provide an appropriate solvent to facilitate isoprene trapping (Bentley and Melis 2012). The 12-carbon alkene retains the isoprene through hydrophobic interactions. One trap was connected with PTFE tubing to a bubbling flask containing an isoprene producing cyanobacteria strain (2MEP-IspS2, Englund *et al* 2018) and the other trap was connected to a bubbling flask containing a control strain (pEEC). Pre-cultures of the two *Synechocystis* strains were grown in BG-11 supplemented with 50 mM HEPES-NaOH, pH 8.0, 20 µg/ml chloramphenicol and 50 mM $NaHCO_3$ at 30°C under 60 µmol m^{-2} s^{-1} continuous white light, for 7 days. The pre-cultures were then diluted with BG-11 to an OD750 of 0.2 before inoculation of the bubbling flasks. Stirring of the culture was provided through vigorous aeration with sterile filtered air. From each of the bubbling flasks containing dodecane, 500 µl samples were taken and placed in GC vials that were then incubated at 37°C for 40 min. After incubation, the headspace of the vials was analysed using GC. The isoprene content of the dodecane was later analysed using capillary GC. Ice packs were continuously replaced to maintain a low temperature in the gas trap.

After 9 days of cultivation, no isoprene could be detected in the dodecane. The open system presented here does not seem to be optimal for isoprene capture. The volatile nature of isoprene, as well as the relatively low production titers of the production strain, means that the vapor pressure of isoprene in the system is extremely low. Henry's law states that the amount of dissolved gas in a liquid is proportional to its partial pressure above the liquid. Since there is a constant gas flow in the open system, the partial pressure of isoprene above the dodecane might be too low for capture. Capturing isoprene requires a system where the partial pressure

of isoprene is high enough or the temperature low enough to facilitate condensation or trapping in a solvent. Constantly cooling the gasses from the PBR for the entire cultivation period is ineffective and expensive. An alternative to growing cultures during constant aeration and harvesting isoprene continuously is to grow cells in a closed PBR where harvesting can be done intermittently. This means that the total volume processed will be lower and the partial pressure of isoprene higher.

3.3.3 Intermittently flushed gas trap systems

Following the continuous harvesting system, another approach was taken. To increase the partial pressure of produced isoprene, cultivation was done in completely sealed PBRs (Figure 17). The cells were provided with carbon by filling the headspace of the reactor with 100% CO_2 before sealing the PBR. This strategy was based on the work done by Bentley and Melis (2012).

A 7 L PBR (Figure 17) was constructed from a glass culture flask sealed with a rubber stopper. Four glass tubes were fitted through the stopper forming designated entrances and exits to and from the reactor. The PBR was inoculated with a 7 L culture with an OD750 of 0.13 of the isoprene-producing 2MEP-IspS2 *Synechocystis* strain. The carbon source for the cells was provided through spontaneous diffusion of headspace CO_2 facilitated by mechanical mixing with a magnetic stirrer. Carbon was also provided by $NaHCO_3$ present in the BG-11 medium. The carbon source availability for the cells is therefore a dynamic and complex combination of the equilibrium between the $NaHCO_3$ concentration, the dissolved CO_2 in the medium and the diffusion of CO_2 from gas to liquid phase. Initially, gaseous CO_2 was added to the reactor by bubbling the bottom of the culture with 100% CO_2 using mass flow controllers at a flow rate of 100 mL/min for 40 min. This was sufficient to completely fill the 4 L headspace with CO_2 gas. The reactor was cultivated at 30°C in 100 µmol m^{-2} s^{-1} white light and flushed every 4 days with CO_2 to push out the gasses that had accumulated in the headspace. The outflow of gasses was directed through a cold trap consisting of two condensers connected in series. The purpose of the first condenser was to condense water vapor and pre-chill the produced isoprene gas. The second was meant to concentrate isoprene vapor and trap it in a two-neck flask that could then be sampled and analysed with GC.

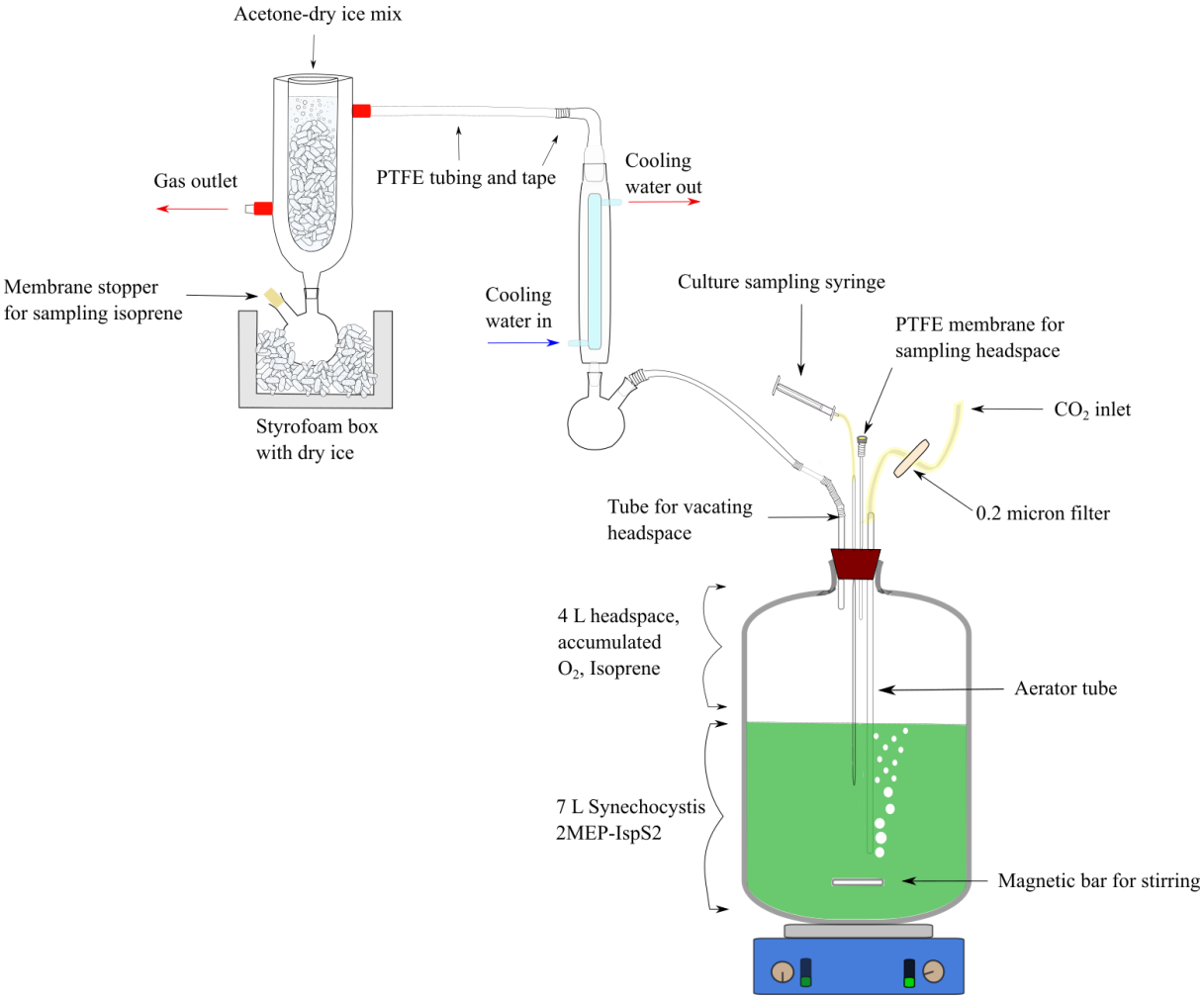

Figure 17: Closed PBR/cold-trap system designed for isoprene production and trapping. The 7 L PBR was slowly fed 100% CO_2 gas through an aerator tube to completely fill the headspace and then the PBR was sealed. Gas exchange between headspace CO_2 and photosynthetically produced O_2 was facilitated by continuous mechanical mixing. This also kept the cells suspended and evenly illuminated in the culture. Cell samples were taken using a syringe connected to a glass tube submerged in the culture. Gas samples of the headspace were taken through a PTFE membrane using a Hamilton syringe that could be directly analysed by gas chromatography (GC). The PBR connects to the two-condenser cold-trap setup with PTFE tubing. The first condenser is cooled with chilled water at 4°C, the second with a dry-ice/acetone mix at -77°C. Connected to the second condenser is a two-neck flask submerged in dry-ice with a septum stopper which enables sampling of trapped isoprene. The system was checked for leaks by connecting a flowmeter to the outflow of the PBR and to the outflow of the gas trap. This flow was compared to the flow of the gas source. Not everything in the figure is to scale.

The 7 L reactor grew for a total of 26 days to a final OD750 of 1.42. During the first 8 days of cultivation the cells grew linearly (Figure 18). From day 9 and forward the growth rate decreased, stagnated and eventually the culture suffered significant cell death. This can be attributed to a decrease in illumination from day 8 that was discovered late in the experiment. However, increased illumination restored and enhanced cell division.

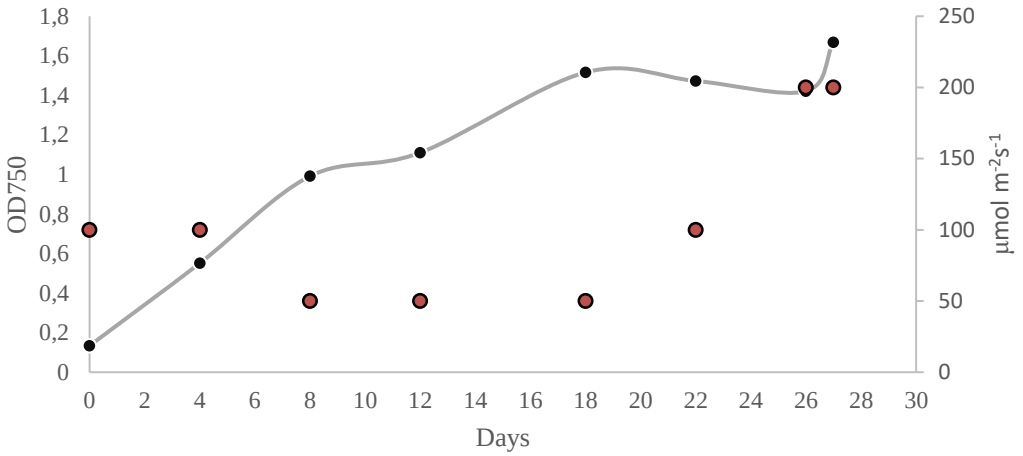

Figure 18: Growth curve of the 7 L PBR. OD750 samples were taken every 4 or 6 days in conjunction with CO_2 flushing up to day 22 and then taken on day 26 and 27 without flushing. Left Y-axis represents cell density (black circles) and right Y-axis white light illumination (red circles). The white light illumination from day 8 to 18 is an approximation.

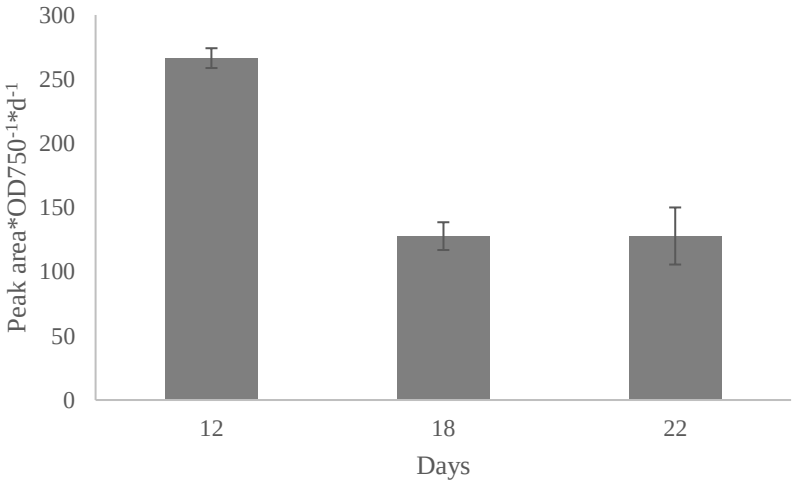

Figure 19: Peak areas of isoprene sampled from the cold trap after flushing the 11L PBR. The Y-axis represents isoprene peak area per day between flushing events normalized to OD750. The first two timepoints, day 4 and 8, are not included to the absence of nitrogen and hydrogen gas for the GC and due to an acetone contamination in the trap obstructing the isoprene peak. The day 26 timepoint could not be measured due to inconsistencies in GC carrier gas. The headspace of the PBR was sampled and run in GC before flushing with CO_2. All measurements were done in technical triplicates.

From the 8th day flushing, an isoprene concentration corresponding to a peak area of 2848 was measured from the PBR headspace. Unfortunately, due to an acetone contamination, the captured isoprene in the trap could not be quantified. For the remaining days, there were measurable amounts of isoprene detected in the gas trap (Figure 19). Interestingly, before flushing, no isoprene could be detected in the headspace of the PBR. This indicates that the cold trap system is able to successfully concentrate isoprene gas.

Due to the fact that the reactor is a closed system and isoprene is accumulated in the headspace, Henry's law suggests that some isoprene will be dissolved in the culture. Hence, when taking isoprene samples from the headspace some isoprene will be dissolved in the culture and will not be represented. When flushing the reactor, the partial pressure of isoprene over the culture will decrease and dissolved isoprene will escape into the gas phase, thus adding more isoprene to the system for potential capture/condensation. In order to evaluate the productivity of the system, both the gaseous and dissolved isoprene must be accounted for. The solubility of a gas in a liquid at a certain pressure is described by equation (1) (Payne *et al*. 2017).

$$C_{liq} = K_H \times P_{gas} \qquad (1)$$

The constant K_H is Henry's constant, a value unique for every gas that describes the gas solubility in a certain liquid. Henry's constant can only be obtained experimentally. Leng and co-workers investigated the solubility of isoprene in water and could determine K_H at 25°C to be 0.036 ± 0.003 mol L^{-1} atm^{-1}. K_H at 30°C can then be calculated using the temperature dependent equation (2) (Leng *et al*. 2013).

$$K_H(T) = K_H(298) \times exp\left[\left(-\frac{\Delta H}{R}\right)\left(\frac{1}{T} - \frac{1}{298}\right)\right] \qquad (2)$$

Here ΔH is the molar enthalpy of solution, T is temperature expressed in kelvin and R is the gas constant. Continuing, the isoprene concentration in the gas phase can be determined using an isoprene standard. The molar fraction of isoprene in the headspace can then be approximated by using the ideal gas law, equation (3), to calculate the total molarity of gasses in the headspace.

$$PV = nRT \qquad (3)$$

Knowing the concentration of isoprene in the headspace, as well as the total molarity, the partial pressure of isoprene is also known. The solubility of isoprene can therefore be verified using equation (1). Using this approach, one could make a rough estimation that 55% of all isoprene in the closed PBR (7:4 culture to headspace volume ratio) is dissolved in the liquid phase. The assumptions needed to make this approximation are; the pressure in the PBR is 1 atm, Henry's constant for isoprene in water is similar to isoprene in BG-11 media, all gaseous molecules in the PBR behave as ideal gases.

A 3.5 L scaled down reactor was constructed to more accurately monitor the growth and isoprene production. The PBR was cultivated at 30°C under 170 µmol m^{-2} s^{-1} continuous white light for 7 days (Figure 20). The PBR was seeded with preculture used for the 7 L reactor that had been regularly refreshed. However, no isoprene was detected in either the headspace or the trap until the 7th day when a peak area of 100 could be detected in the trap.

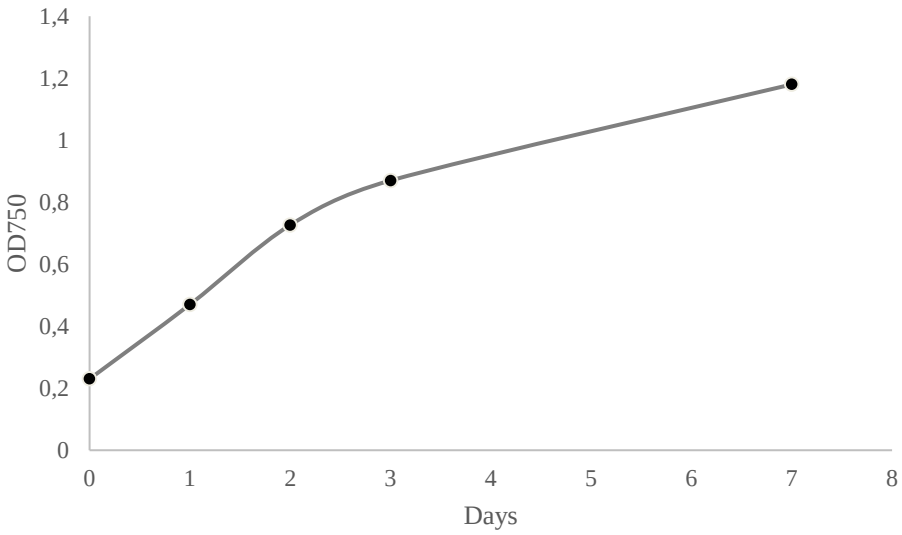

Figure 20: Growth of the 2MEP-IspS2 strain in a 3.5 L reactor. The reactor was flushed to capture isoprene on day 1, 3 and 7. Culture grew under continuous illumination of 170 µmol m^{-2} s^{-1} at 30°C.

An interesting observation that was made while working on both closed reactors was that the pressure in the reactors dropped during cultivation. After only one day of cultivation, the pressure inside the 3.5 L reactor had dropped to 0.8 atm.

4 Discussion

4.1 *In vivo* isobutene production pathway

The goal of this part of the project was to engineer an *in vivo* production pathway of isobutene in cyanobacteria. This was ultimately not feasible under this given timeframe. The isobutene producing capability of Cyt.P450cm could not be validated. From the experiments performed on the thylakoid preparations of the Cyt.P450cm-expressing *Synechocystis* (Figure 6) it is unclear whether the enzyme is functional. The western blot indicates that the protein is located in the thylakoid membrane. It is possible that the preparation contains periplasmic membranes but for cyanobacteria the ratio of thylakoid to periplasmic membrane in the membrane fraction is substantial (Norling *et al*. 1998). Continuing, the results from the *in vitro* isobutene activity assay were inconclusive due to the spontaneous formation of isobutene or a similar compound. It is possible that Cyt.P450cm is correctly incorporated in the thylakoid membrane, is reduced via ferredoxin from the electron transport chain and facilitates isobutene production but has too low of a catalytic rate. The reported turnover rate of Cyt.P450cm is 0.27 min^{-1} (Fukuda *et al*. 1994). In contrast, the reported catalytic rates for IpdC and PadA in *E. coli* are 293 min^{-1} and 1116 min^{-1} respectively (Xiong *et al*. 2012). Even though this cannot be directly translated to rates in cyanobacteria, it indicates that

Cyt.P450cm would be the bottleneck in a fully integrated cyanobacterial pathway of these enzymes.

The discovery that isovalerate spontaneously decomposed to isobutene (or a similar compound) provided an incentive to continue with the *in vivo* pathway even though the Cyt.P450cm productivity remained undetermined. Unfortunately, no reliable quantification method was found. Analysis of isovaleraldehyde and isovalerate using capillary GC was deemed unsuitable as spontaneous decarboxylation at the moment of injection produces a wide array of decomposition products that complicates quantitative and qualitative analysis. Using LC-MS was not applicable either as the molecular weight of the substrates isovalerate and isovaleraldehyde were under the detection limit of the MS. Therefore, an attempt was made to identify isovaleraldehyde and isovalerate by producing unique "fingerprints" of decomposition products from crude extracts. However, the *in vitro* crude extract assay of IpdC and PadA did not yield any conclusive results. All of the distinct peaks observed for the IpdC and PadA samples were also present in the EVC samples. This means that all peaks correspond to decomposition products derived from the added substrate or from a natively produced compound. A future course of action could be to determine enzyme activity using purified IpdC and PadA to eliminate "background noise".

After the *in vitro* activity assay western blots were performed on the same crude extracts (Figure 14). There is clear expression of PadA but no observed expression of IpdC. It is possible that the IpdC-producing *Synechocystis* had lost the gene of interest before performing the *in vitro* activity assay. That would then explain the lack of isovaleraldehyde produced by pEEK2-IpdC crude extracts if isovaleraldehyde would give distinct peaks separated from EVC peaks. In figure 14 the western blot clearly shows that there is no production of the protein although the stained membrane control confirms proper loading. The cells used for the activity assay and the western blot were refreshed from cultures used in the first western blot of *Synechocystis* (Figure 12). It is highly possible that this gave enough time for the cells to discard the *ipdC* gene to become empty vector plasmid carriers.

The enzymes IpdC and PadA were both successfully induced in *E. coli* and resulted in substantial amounts of protein in the soluble fraction (Figure 10). Both IpdC and PadA were also successfully expressed in *Synechocystis*, indicating that the codon optimization resulted in good translational efficiency.

If more work is to be done on the enzymes IpdC and PadA in the context of isobutene production, the spontaneous decomposition to isobutene needs to be verified. Even though the observed peaks perfectly correspond to the one of an isobutene standard, it is possible that it belongs to a similar molecule such as isobutane. This is crucial information for the purpose of polymerisation. In a study from 1965 Kochi and co-workers examined the heat-induced decarboxylation of isovalerate facilitated by different catalysts, the choice of which, influenced the isomerisation of the product mix (Kochi 1965). For example, in the presence of pyridine, isobutane was formed in 35% yield and isobutene in only 1% yield. It is also worth

to mention that among their results was the observed inhibition of decarboxylation in the presence of oxygen. In cyanobacterial cells exists a myriad of potential catalysts along with a continuous production of oxygen through photosynthesis. Taking this into account, specific and efficient production of isobutene through spontaneous decarboxylation seems unlikely.

One thing to mention was that PadA differed from the expected size given in literature (Ferrández *et al*. 1997). Western blots of *E coli* as well as *Synechocystis* clearly show a protein that exceeds the expected size with several kD. The added size due the Strep-II tag is unlikely to be the cause as it is only 1 kD. There are many factors that can influence the mobility of a protein in the gel like structural compactness, differential SDS binding and net charge (Tung and Knight 1972).

4.1.1 Conclusions

The results from this work highlights that further research is needed to accurately determine the isobutene-producing capability of Cyt.P450cm in cyanobacteria using more precise means of product quantification. Continuing, even though the activities of IpdC and PadA has previously been examined in *E. coli*, their heterologous function in *Synechocystis* must be determined. Without specific catalysis of isovalerate by Cyt.P450cm, the purity of spontaneously obtained isobutene needs to be verified.

4.2 Photobioreactor and gas-trap systems

The goal of this part of the project was to construct a photo-bioreactor with a gas-harvesting system that was capable of production and collection of cyanobacterial isoprene. The work also included the identification of materials suitable for this purpose. In this report is an evaluation of a closed PBR/cold-trap system that was able to concentrate isoprene to measurable amounts. Materials such as silicone rubber was shown to be completely incompatible with such a system due to substantial losses of gas.

The GC results from the first large PBR shows that the cold trap system was able to concentrate isoprene vapour to measurable concentrations. Unfortunately, the results could not be replicated with smaller scale reactors. It is possible that by regularly refreshing precultures for the PBRs instead of starting fresh culture from frozen stocks, the productivity of the isoprene producing strain decreased. This in combination with the decrease in culture volume and inevitable losses in the system due to isoprene diffusion (Figure 16) might have led to isoprene concentrations being under the detection limit. In the 7 L PBR, the production of isoprene decreased sharply after day 8. This could be attributed to the decrease in illumination in combination with increased light attenuation due to higher culture density.

From this work I would tentatively suggest that an intermittently flushed PBR system holds the advantage over continuously grown systems with the purpose of volatile hydrocarbon production. The cyanobacteria are capable of growing in a 100% CO_2 atmosphere in closed PBRs. The increase in headspace concentrations of *e.g.* isoprene facilitates harvesting which

can be performed when appropriate. However, since the production titers of isoprene remain fairly low (Englund *et al*. 2018), the harvesting system needs to be scaled according to production. Regarding the PBR itself, for lab-scale production purposes, a cylindrical cultivation vessel is likely sufficient. However, for large-scale production of isoprene the reactor design needs to address the issues associated with large volumes. These include light attenuation, mixing and feeding of fresh cultivation media (Johnson *et al*. 2018, Kumar *et al*. 2011). The latter is especially important for longer cultivation periods and is something to be considered at lab-scale.

In the system described in this work the scale of the gas-harvesting system is likely oversized for the productivity of the isoprene producing cyanobacteria. The volume of the condenser might be too large for efficient heat transfer between the isoprene and condenser. Therefore, a potential way of increasing the capture yield of the cold trap system is to increase the internal surface area to gas ratio of the condenser. This could be done by leading the gas from the PBR through a thin metal coil submerged in a coolant. Using this approach, a larger fraction of gas will be in constant contact with a cooling surface and the longer path will increase the total time that the gas is being cooled. Continuing, bubbling the gas through a hydrophobic solvent increases the amount of retained isoprene through chemical intermolecular interactions (Kim *et al*. 2016). This approach was not explored in conjunction with the dry-ice system due to safety concerns. The solvents appropriate for dissolving isoprene are mostly flammable and in a system of large temperature differences, the risk is increased. As the system was designed, the harvesting of isoprene was depending on the condensation of isoprene vapour and the collection of liquid isoprene in a vessel.

The very volatile nature of isoprene makes the compound extremely difficult to work with. Rapid evaporation of liquid isoprene to gas complicates the matter of maintaining accurate standards. Common laboratory equipment such as membrane stoppers and tubing are predominantly made from rubbers capable of absorbing short volatile hydrocarbons like isoprene. To minimize losses of isoprene in the PBR/cold-trap system, all connections, tubing and valves must be made of inert materials such as; PTFE, glass or metal. In the system described in this work, all connections; glass to silicone tubing or PTFE tubing to silicone tubing were wrapped in PTFE tape in an attempt to reduce the amount of escaped isoprene. However, there are still significant losses of isoprene as evidenced by the small-scale experiment described in Figure 15.

For future work with closed PBRs, for correct calculations of yields of a given production system, the amount of dissolved gas in the media needs to be taken into account. Herein lies a suggested approach to approximate the amount of dissolved isoprene in closed PBR system. However, for more precise approximations, the gas solubility constant should be determined experimentally in BG-11 media at certain temperatures.

In order to advocate for the potential of the production system described here, one has to address the issue of obtaining a sustainable carbon source for efficient cyanobacterial growth.

Globally, the largest sources of CO_2 emissions are from combustion of fossil fuels. The flue gas that is emitted from fossil fuel sources are comprised mostly of N_2, O_2 and H_2O with smaller amounts of CO, NO_x, SO_x and microscopic particulate matter (Kumar *et al*. 2011). An alternative to fossil-derived flue gas is to use flue gas produced from the paper and pulp industry. In Sweden, 65% of all CO_2 emissions are from biogenic sources, 46% is emitted from the paper and pulp industry (Hansson *et al*. 2017). CO_2 from this source could be used to flush cyanobacterial cultures and in the context of volatile hydrocarbon harvesting, recirculated to increase harvesting yields and minimize CO_2 emissions.

There was the issue of GC performance through a large portion of the project, fluctuating or lack of gasses. This meant that there were no proper isobutene or isoprene standards made to quantify production. It is also unknown if the sensitivity of the GC detector (FID) remained stable during this period.

4.2.1 Conclusions

This work has been a proof of concept to show the possibility of harvesting isoprene produced by cyanobacteria. Highlighted are the issues associated with common laboratory materials. Going forward, there is the need for an optimized harvesting system scaled according to current production levels.

5 Acknowledgements

I would like to thank my supervisor Karin Stensjö for giving me the opportunity to work on this project and always providing support when needed. Thank you Henna Mustila and João Rodrigues for being great secondary supervisors and guiding me in the lab. Thanks to Anup Rana and the members of the Jet fuel group. To all the people working in the cyano group, thank you for being so welcoming and answering any and all questions I had.

Special thanks to my wonderful parents who provided so much support, especially throughout the last few weeks of the project.

References

Bentley FK, Melis A. 2012. Diffusion-based process for carbon dioxide uptake and isoprene emission in gaseous/aqueous two-phase photobioreactors by photosynthetic microorganisms. Biotechnology and Bioengineering 109: 100–109.

Chaves JE, Melis A. 2018. Biotechnology of cyanobacterial isoprene production. Applied Microbiology and Biotechnology 102: 6451–6458.

Chou C-C, Riviere JE, Monteiro-Riviere NA. 2002. Differential Relationship between the Carbon Chain Length of Jet Fuel Aliphatic Hydrocarbons and Their Ability to Induce Cytotoxicity vs. Interleukin-8 Release in Human Epidermal Keratinocytes. Toxicological Sciences 69: 226–233.

Englund E, Liang F, Lindberg P. 2016. Evaluation of promoters and ribosome binding sites for biotechnological applications in the unicellular cyanobacterium Synechocystis sp. PCC 6803. Scientific Reports 6: 36640.

Englund E, Shabestary K, Hudson EP, Lindberg P. 2018. Systematic overexpression study to find target enzymes enhancing production of terpenes in Synechocystis PCC 6803, using isoprene as a model compound. Metabolic Engineering 49: 164–177.

Ferrandez A, Prieto MA, Garcia JL, Diaz E. 1997. Molecular characterization of PadA, a phenylacetaldehyde dehydrogenase from Escherichia coli. FEBS letters 406: 23–27.

Fukuda H, Fujii T, Sukita E, Tazaki M, Nagahama S, Ogawa T. 1994. Reconstitution of the isobutene-forming reaction catalyzed by cytochrome P450 and P450 reductase from Rhodotorula minuta: decarboxylation with the formation of isobutene. Biochemical and Biophysical Research Communications 201: 516–522.

Gao X, Gao F, Liu D, Zhang H, Nie X, Yang C. 2016. Engineering the methylerythritol phosphate pathway in cyanobacteria for photosynthetic isoprene production from CO2. Energy & Environmental Science 9: 1400–1411.

Hansson J, Hackl R, Taljegard M, Brynolf S, Grahn M. 2017. The Potential for Electrofuels Production in Sweden Utilizing Fossil and Biogenic CO2 Point Sources. Frontiers in Energy Research, doi 10.3389/fenrg.2017.00004.

Johnson TJ, Katuwal S, Anderson GA, Gu L, Zhou R, Gibbons WR. 2018. Photobioreactor cultivation strategies for microalgae and cyanobacteria. Biotechnology Progress 34: 811–827.

Kim J-H, Wang C, Jang H-J, Cha M-S, Park J-E, Jo S-Y, Choi E-S, Kim S-W. 2016. Isoprene production by Escherichia coli through the exogenous mevalonate pathway with reduced formation of fermentation byproducts. Microbial Cell Factories, doi 10.1186/s12934-016-0612-6.

Kochi JK. 1965. Oxidation with Lead(IV). I. Mechanism of the Decarboxylation of Pentanoic Acids. Journal of the American Chemical Society 87: 3609–3619.

Kumar K, Dasgupta CN, Nayak B, Lindblad P, Das D. 2011. Development of suitable photobioreactors for CO2 sequestration addressing global warming using green algae and cyanobacteria. Bioresource Technology 102: 4945–4953.

van Leeuwen BNM, van der Wulp AM, Duijnstee I, van Maris AJA, Straathof AJJ. 2012. Fermentative production of isobutene. Applied Microbiology and Biotechnology 93: 1377–1387.

Leng C, Kish JD, Kelley J, Mach M, Hiltner J, Zhang Y, Liu Y. 2013. Temperature-dependent Henry's law constants of atmospheric organics of biogenic origin. The Journal of Physical Chemistry A 117: 10359–10367.

Liang F, Englund E, Lindberg P, Lindblad P. 2018. Engineered cyanobacteria with enhanced growth show increased ethanol production and higher biofuel to biomass ratio. Metabolic Engineering, doi 10.1016/j.ymben.2018.02.006.

Lindberg P, Park S, Melis A. 2010. Engineering a platform for photosynthetic isoprene production in cyanobacteria, using Synechocystis as the model organism. Metabolic Engineering 12: 70–79.

Meeks JC, Castenholz RW. 1971. Growth and photosynthesis in an extreme thermophile, Synechococcus lividus (Cyanophyta). Archiv Fur Mikrobiologie 78: 25–41.

Miao R, Liu X, Englund E, Lindberg P, Lindblad P. 2017. Isobutanol production in Synechocystis PCC 6803 using heterologous and endogenous alcohol dehydrogenases. Metabolic Engineering Communications 5: 45–53.

Miao R, Xie H, Lindblad P. 2018. Enhancement of photosynthetic isobutanol production in engineered cells of Synechocystis PCC 6803. Biotechnology for Biofuels, doi 10.1186/s13068-018-1268-8.

Mutalik VK, Guimaraes JC, Cambray G, Lam C, Christoffersen MJ, Mai Q-A, Tran AB, Paull M, Keasling JD, Arkin AP, Endy D. 2013. Precise and reliable gene expression via standard transcription and translation initiation elements. Nature Methods 10: 354–360.

Norling B, Zak E, Andersson B, Pakrasi H. 1998. 2D-isolation of pure plasma and thylakoid membranes from the cyanobacterium Synechocystis sp. PCC 6803. FEBS Letters 436: 189–192.

Rossoni L, Hall SJ, Eastham G, Licence P, Stephens G. 2015. The Putative Mevalonate Diphosphate Decarboxylase from Picrophilus torridus Is in Reality a Mevalonate-3-Kinase with High Potential for Bioproduction of Isobutene. Appl Environ Microbiol 81: 2625–2634.

Parmar A, Singh NK, Pandey A, Gnansounou E, Madamwar D. 2011. Cyanobacteria and microalgae: a positive prospect for biofuels. Bioresource Technology 102: 10163–10172.

Payne B. 2017. Chapter Eleven - Henry's Law and Monitoring Methane in Groundwater Wells. In: Schug KA, Hildenbrand ZL (ed.). Advances in Chemical Pollution, Environmental Management and Protection, pp. 275–319. Elsevier,

Singh A, Upadhyay V, Upadhyay AK, Singh SM, Panda AK. 2015. Protein recovery from inclusion bodies of Escherichia coli using mild solubilization process. Microbial Cell Factories, doi 10.1186/s12934-015-0222-8.

Tung J-S, Knight CA. 1972. Relative importance of some factors affecting the electrophoretic migration of proteins in sodium dodecyl sulfate-polyacrylamide gels. Analytical Biochemistry 48: 153–163.

Wilson J, Gering S, Pinard J, Lucas R, Briggs BR. 2018. Bio-production of gaseous alkenes: ethylene, isoprene, isobutene. Biotechnology for Biofuels 11: 234.

Wlodarczyk A, Gnanasekaran T, Nielsen AZ, Zulu NN, Mellor SB, Luckner M, Thøfner JFB, Olsen CE, Mottawie MS, Burow M, Pribil M, Feussner I, Møller BL, Jensen PE. 2016. Metabolic engineering of light-driven cytochrome P450 dependent pathways into Synechocystis sp. PCC 6803. Metabolic Engineering 33: 1–11.

Xiong M, Deng J, Woodruff AP, Zhu M, Zhou J, Park SW, Li H, Fu Y, Zhang K. 2012. A Bio-Catalytic Approach to Aliphatic Ketones. Scientific Reports, doi 10.1038/srep00311.

Zhang Y, Yang B, Li K, Hou D, Zhao C, Wang J. 2017. Electrospun porous poly(tetrafluoroethylene-: Co -hexafluoropropylene- co -vinylidene fluoride) membranes for membrane distillation. RSC Advances 7: 56183–56193.

Supplementary A. Cyt.P450cm activity assay

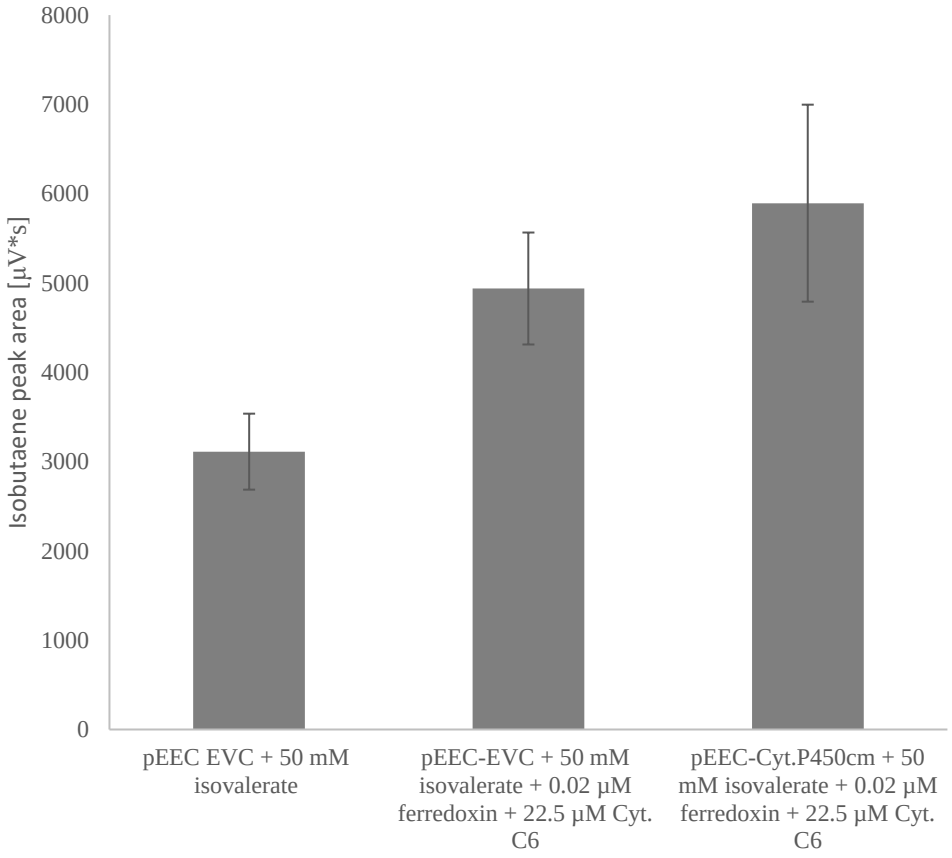

Figure S1: Cyt.P450 activity assay with twice the amount of ferredoxin as the assay described in figure 5. Viability of thylakoid membranes not evaluated through oxygen evolution experiments. Incubation time 15 h at 30°C.

Supplementary B. pEEK2-IpdC plasmid

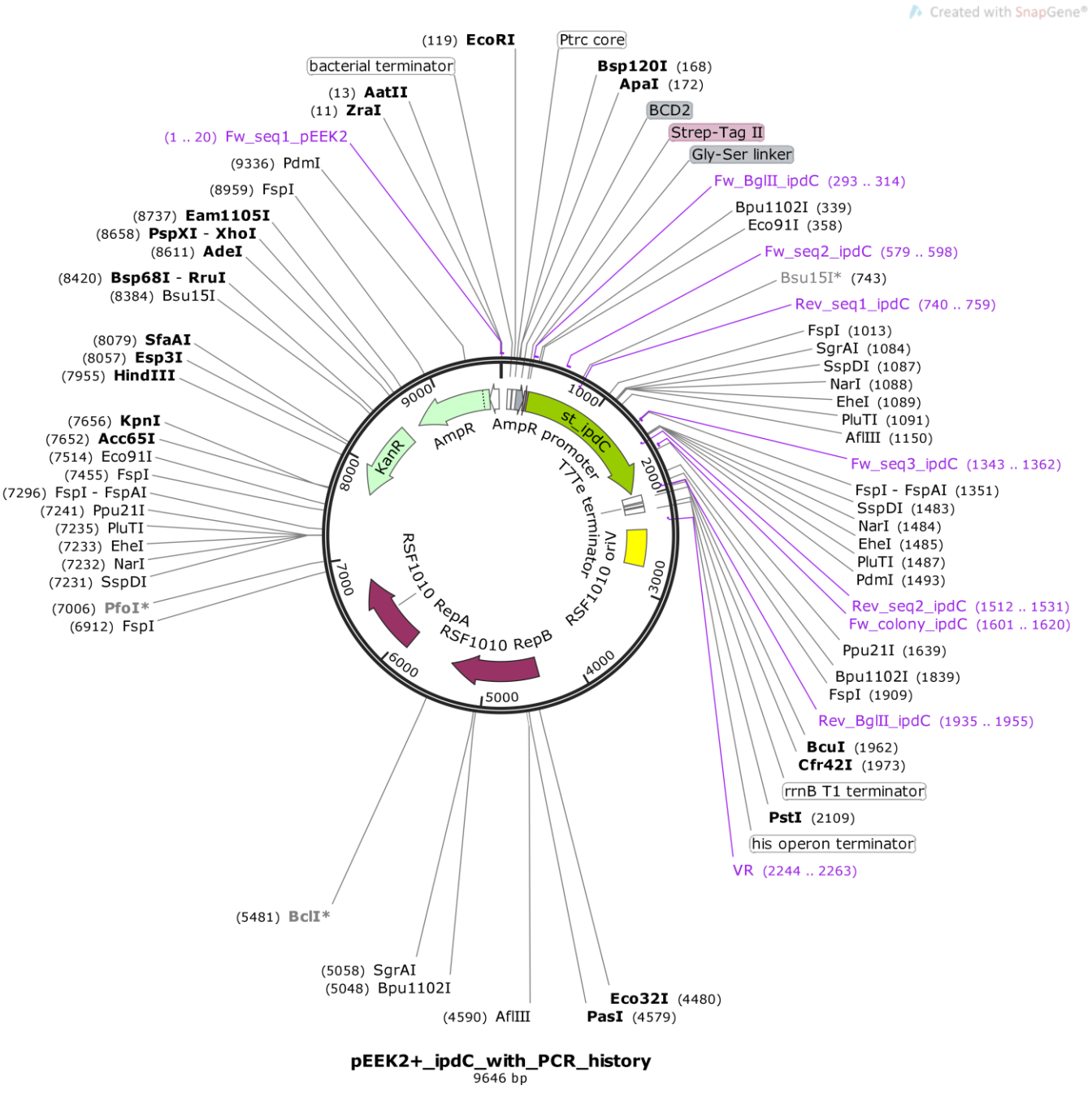

Figure S2: SnapGene map of the *ipdC* genetic construct.

Supplementary C. pEEK2-PadA plasmid

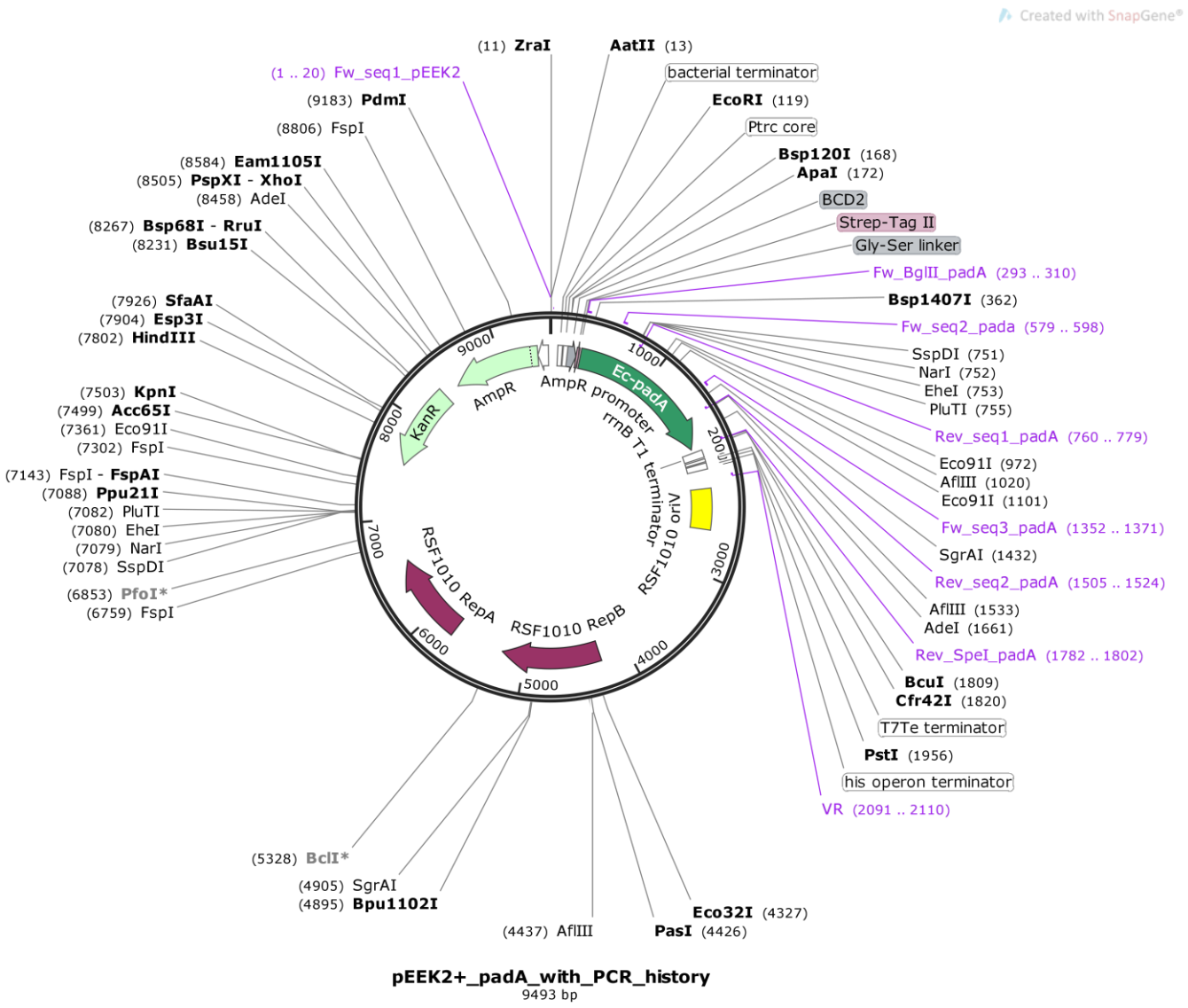

Figure S3: SnapGene map of the *padA* genetic construct.

Supplementary D. Primers used in this work

Table S1: Primers used in this work.

Primer	5´->3´
Fw_seq1_pEEK2	TGCCACCTGACGTCTAAGAA
Rev_seq1_ipdC	GCCAAGAACGCGATCGATTT
Fw_seq2_ipdC	CCCGGTTTTACATATTGTGG
Rev_seq2_ipdC	GAGAGTAACCAATAGACCCC
Fw_seq3_ipdC	AACCAGTGCGCATTGACAAA
Rev_seq1_padA	TTCCTAGTCCAGGCCTGATA
Fw_seq2_pada	TGAACAACATTCCGAAGAAT
Rev_seq2_padA	CACAACAGGACCAAAAACTT
Fw_seq3_padA	CCCATTGTGACAAAGTTTGT
VR	ATTACCGCCTTTGAGTGAGC

Supplementary E. BG-11 recipe

Table S2: BG-11 supplemented with 50 mM HEPES recipe.

dH_2O	934 mL
HEPES (1M)	50 mL
$NaNO_3$(100x)	10 mL
K_2HPO_4	40 mg
$MgSO_4*7H_2O$	75 mg
$CaCl_2*2H_2O$	36 mg
Citric acid	6 mg
Ferric ammonium citrate	6 mg
EDTA disodium salt	1 mg
Na_2CO_3	20 mg
H_3BO_3	2.86 mg
$MnCl_2*4H_2O$	1.81 mg
$ZnSO_4*7H_2O$	0.222 mg
Na_2MoO_4	0.395 mg
$CuSO_4*5H_2O$	0.0790 mg
$Co(NO_3)2*6H_2O$	0.0494 mg

Supplementary F. Cloning strategy

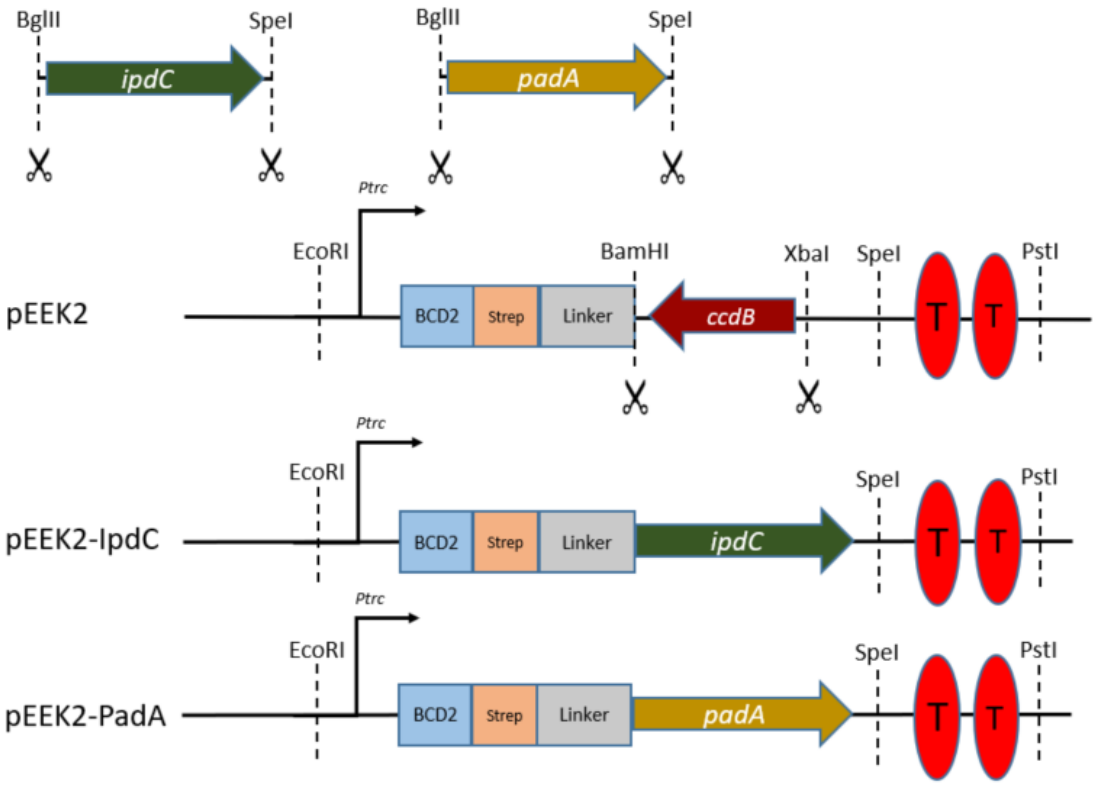

Figure S4: Cloning strategy of *ipdC* and *padA* genes.

Supplementary G. Colony PCR

Table S3: Colony PCR program and recipe for a 20 µl reaction.

STEP	**TEMP**	**TIME**
Initial Denaturation	95°C	3 min
Denaturation	95°C	30 seconds
Annealing	Tm-5	30 seconds
Extension	72°C	1 min per 2 kb
Final Extension	72°C	5 minutes
Hold	12°C	
25-35 Cycles		

10x DreamTaq buffer	2 µl
10 mM dNTPs	0.5 µl
Forward primer (10 µM)	1 µl
Reverse primer (10 µM)	1 µl
DreamTaq DNA Pol.	0.2 µl
dH_2O	15 µl
Template DNA (200 -400 ng)	2 µl